UNIVERSITÀ DEGLI STUDI DI TRIESTE

# UNIVERSITÀ DEGLI STUDI DI TRIESTE

## XXXIV CICLO DEL DOTTORATO DI RICERCA IN
SCIENZE DELLA RIPRODUZIONE E DELLO SVILUPPO

# PACSIN2 as a modulator of autophagy and thiopurine sensitivity: in vitro evaluations in lymphoid and intestinal cells

Settore scientifico-disciplinare: **BIO/14**


DOTTORANDA
**GIULIA ZUDEH**

COORDINATORE
**PROF. PAOLO GASPARINI**

SUPERVISORE DI TESI
**PROF. GABRIELE STOCCO**


**ANNO ACCADEMICO 2020/2021**

*ABSTRACT* 3

*RIASSUNTO* 5

1. Thiopurines 7
   - 1.1 Clinical application 7
   - 1.2 Pharmacodynamics 9
   - 1.3 Pharmacokinetics 11
   - 1.4 Adverse reactions 12
   - 1.5 Pharmacogenetics 12
   - 1.6 Other possible biomarkers of thiopurines response 13
2. PACSIN2 15
3. Autophagy 16
   - 3.1 Autophagy machinery 18
   - 3.2 Autophagy markers 20
   - 3.3 LIR domain 21
4. Apoptosis 22
   - 4.1 PARP1 24

*AIM* 25

*MATERIAL AND METHODS* 26

1. Cell lines 26
2. Treatments 26
3. Patients' samples 28
4. Cell lysates preparation 28
5. Immunoblotting 29
6. RNA extraction 30
7. Gene expression analysis 30
8. LC3 interacting region (LIR) identification 30
9. Plasmids expansion and purification 31
10. Transient cell transfection 32
11. Co-immunoprecipitations 32
12. Drug sensitivity assay 33
13. Mitochondrial membrane potential measurement 33
14. HPLC-UV analysis 33
15. Statistical analysis 34

*RESULTS* 35

1. Cell line characterization 35
2. Autophagy is increased after *PACSIN2* KD 36
3. *PACSIN2* could play a role in first phases of autophagy 38

4. **Colon samples of IBD pediatric patients showed an inverse correlation among PACSIN2 amount and both inflammation and autophagy levels** 38
5. ***In silico* identification of the LIR domain present in PACSIN2** 39
6. **PACSIN2-LC3 protein-protein interaction: experimental validation** 40
7. ***PACSIN2* KD affects the unfolded protein stress response, evaluated as tunicamycin sensitivity** 41
8. ***PACSIN2* KD impact on thiopurine sensitivity** 43
9. ***PACSIN2* KD counteracts mercaptopurine-induced autophagy inhibition** 44
10. **Both mercaptopurine treatment and *PACSIN2* KD increased apoptosis in intestinal cells** 45
11. ***PACSIN2* KD did not impact on thiopurine metabolites TGN and MMPN concentrations in LS180 cells** 48
12. **PACSIN2 modulated TPMT activity through a molecular mechanism different from autophagy** 49

***DISCUSSION*** 52

***CONCLUSION AND FUTURE AIMS*** 57

***REFERENCES*** 58

# ABSTRACT

Thiopurines, such as mercaptopurine and azathioprine, are leukotoxic agents used to treat acute lymphoblastic leukemia (ALL) and inflammatory bowel disease (IBD). Thiopurine-methyltransferase (TPMT) is an enzyme involved in thiopurine inactivation; its function is affected mainly by known *TPMT* polymorphisms and by Protein Kinase C And Casein Kinase Substrate In Neurons 2 (PACSIN2) through a less characterized molecular mechanism. The rs2413739 variant in *PACSIN2* is an expression quantitative trait locus (eQTL) associated with severe gastrointestinal effects of mercaptopurine in childhood ALL and with azathioprine efficacy in IBD pediatric patients through an uncharacterized mechanism that could be related to autophagy.

The present study aims to clarify the role of PACSIN2 in autophagy and in thiopurine cytotoxicity in leukemic and intestinal models. Moreover, this project aims to evaluate the possible effect of both mercaptopurine exposure and *PACSIN2* KD on both autophagy and apoptosis induction in an intestinal model.

Leukemic (NALM6) and intestinal (LS180) cells with *PACSIN2* knock-down (KD) showed higher autophagy, assessed as LC3-II and SQSTM1/P62 amount. Autophagy flux analysis by chloroquine treatment showed increased LC3-II and SQSTM1/P62 amount, suggesting that PACSIN2 affects the early autophagy phases. The inverse association between PACSIN2 amount and autophagy levels was observed also in inflamed compared to non-inflamed colon biopsies of IBD pediatric patients, confirming the *in vitro* results. No significant association between TPMT amount and autophagy levels was detected, indicating that modulation of autophagy is not the molecular mechanism at the basis of PACSIN2 impact on TPMT activity. Moreover, HPLC-UV analysis showed that PACSIN2 did not affect mercaptopurine pharmacokinetics on intestinal *in vitro* models.

PACSIN2 has a LC3 interacting region (LIR) motif and co-immunoprecipitation analysis confirms that PACSIN2 binds LC3. Transient expression of PACSIN2 with a mutated LIR motif reduced the level of co-immunoprecipitated LC3, showing a role of the LIR motif of PACSIN2 in the interaction.

*PACSIN2* KD increased mercaptopurine sensitivity in LS180 but not in NALM6 cells, suggesting a tissue specific role of PACSIN2 in the intestine after mercaptopurine treatment. Interestingly, mercaptopurine exposure reduced autophagy levels, but *PACSIN2* KD counteracted this effect; moreover, both mercaptopurine exposure and *PACSIN2* KD are able to stimulate apoptosis.

Taken together, these results demonstrate for the first time a clear role of PACSIN2 as an inhibitor of autophagy, putatively through inhibition of autophagosome formation by a protein-protein interaction with LC3-II mediated by a LIR motif present in the PACSIN2 sequence. Moreover, *in vitro* evidences of the role of PACSIN2 as a modulator of mercaptopurine-induced cytotoxicity in intestinal cells

were provided, suggesting that PACSIN2-regulated autophagy levels might influence thiopurine sensitivity.

# RIASSUNTO

Le tiopurine, come la mercaptopurina e l'azatioprina, sono agenti leucotossici usati per trattare la leucemia linfoblastica acuta (LLA) e le malattie infiammatorie croniche intestinali (MICI). La tiopurina-metiltransferasi (TPMT) è un enzima coinvolto nell'inattivazione delle tiopurine; la sua funzione è influenzata principalmente dalle varianti geniche di *TPMT* e di Protein Kinase C And Casein Kinase Substrate In Neurons 2 (PACSIN2). La variante rs2413739 in *PACSIN2* è considerata un expression quantitative trait locus (eQTL) associato a gravi effetti gastrointestinali da mercaptopurina in pazienti pediatrici con LLA infantile e all'efficacia dell'azatioprina in pazienti pediatrici affetti da MICI attraverso un meccanismo non caratterizzato, che potrebbe essere correlato all'autofagia.

Il presente studio mira a chiarire il ruolo di PACSIN2 nell'autofagia e nella citotossicità delle tiopurine in modelli linfoidi ed intestinali. Inoltre, questo progetto mira a valutare il possibile effetto dell'esposizione a mercaptopurina e del silenziamento di PACSIN2 sia sull'autofagia che sull'apoptosi in un modello cellulare intestinale.

I risultati ottenuti sulle linee cellulari immortalizzate linfoidi (NALM6) ed intestinali (LS180) con il silenziamento stabile (knock-down, KD) di *PACSIN2* hanno identificato livelli autofagici maggiori, valutati tramite quantificazione dei livelli dei marcatori autofagici LC3-II e SQSTM1/P62, indicando il possibile ruolo di PACSIN2 come modulatore negativo delll'autofagia. È stata svolta un'analisi del flusso autofagico mediante trattamento con clorochina, che ha mostrato un aumento della quantità di LC3-II e SQSTM1/P62, suggerendo il coinvolgimento di PACSIN2 nella regolazione delle prime fasi dell'autofagia. Inoltre, la correlazione inversa tra la quantità di PACSIN2 ed i livelli autofagici è stata osservata anche in un gruppo di biopsie di tratti infiammati del colon rispetto a biopsie di colon non infiammato di pazienti pediatrici con MICI, confermando i risultati ottenuti *in vitro*.

Non è stata rilevata alcuna associazione significativa tra la quantità di TPMT e i livelli dei marcatori autofagici, indicando che la modulazione di PACSIN2 sull'attività di TPMT possa coinvolgere meccanismi diversi dall'autofagia. Inoltre, analisi HPLC-UV hanno dimostrato che PACSIN2 non influenza la farmacocinetica della mercaptopurina sulle linee cellulari intestinali.

È stata identificata un'interazione proteina-proteina tra PACSIN2 e LC3, mediata da un dominio di legame a LC3 presente nella sequenza amminoacidica di PACSIN2.

Infine, è stato dimostrato che il silenziamento di PACSIN2 è correlato ad una maggior sensibilità alla mercaptopurina nelle cellule LS180 ma non nelle cellule NALM6, suggerendo un ruolo tessuto specifico di PACSIN2 nell'intestino dopo il trattamento con mercaptopurina. È interessante notare come l'esposizione alla mercaptopurina abbia ridotto i livelli autofagici delle cellule LS180 e questo

effetto sia meno evidente nelle cellule con il *PACSIN2* KD; inoltre, sia l'esposizione alla mercaptopurina che il *PACSIN2* KD hanno aumentato i livelli apoptotici delle cellule LS180.

I risultati di questo lavoro dimostrano per la prima volta il ruolo di PACSIN2 come inibitore delle prime fasi dell'autofagia, presumibilmente attraverso il legame del dominio LIR di PACSIN2 a LC3-II. Infine, è stato dimostrato il ruolo di PACSIN2 come modulatore della citotossicità alle tiopurine in modelli cellulari immortalizzati intestinali, suggerendo che i livelli di autofagia regolati da PACSIN2 potrebbero influenzare la sensibilità alle tiopurine.

# INTRODUCTION

## 1. Thiopurines

Thiopurines are antimetabolite drugs presenting an structure analogue to purines (figure 1); in particular, mercaptopurine is an analogue of hypoxanthine, whereas thioguanine is an analogue of guanine. Azathioprine is a prodrug that is converted *in vivo* mainly by a rapid non-enzymatic reaction and by glutathione S-transferase (GST) into its active form: mercaptopurine. (Eklund et al., 2006)

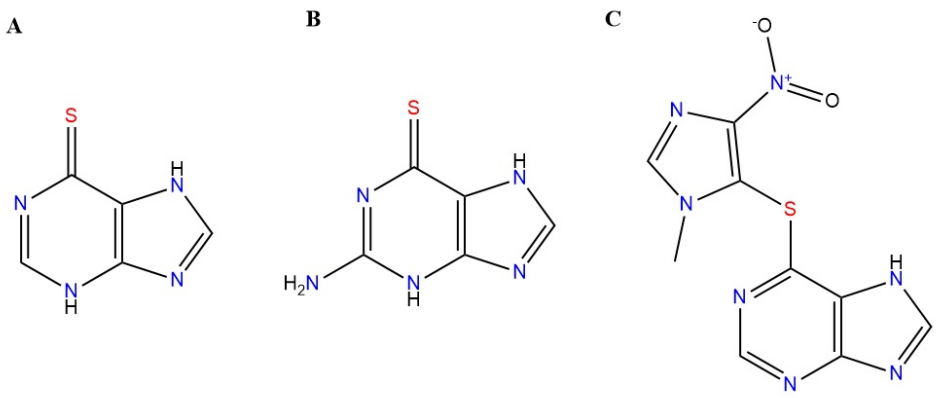


***Figure 1: Thiopurine structure.*** *A) mercaptopurine, B) thioguanine, C) azathioprine*

### 1.1 Clinical application

Thiopurines are used in the treatment of hematological malignancies, such as acute lymphoblastic leukemia (ALL), and in non-malignant conditions, such as inflammatory bowel diseases (IBD). (Relling et al., 2019) (Lamb et al., 2013)

For ALL therapy, thiopurines are used in the context of polychemotherapeutic protocols that include many leukotoxic and cytotoxic drugs, such as glucocorticoids, asparaginase, anthracyclines, vincristine and methotrexate. (Relling & Evans, 2015) (Conter et al., 2010) These therapeutic schemes share the risk-adapted polychemotherapeutic approach. In particular, these

protocols consist in an initial remission-induction phase to eliminate leukemic cells and restore the normal hematopoiesis, followed by a remission-consolidation therapy and then by a long-term maintenance regimen to eradicate the minimal residual tumoral cells. This therapeutic approach has been extremely successful in pediatric patients, leading to a 5-year survival rate greater than 90% in developed countries. (Conter et al., 2010) (Inaba & Pui, 2019) Patient's risk stratification has been based on genetic and clinical factors, such as blasts somatic mutations and chemotherapy response; in particular, the possibility of monitoring levels of the minimal residual disease have improved patient's prognosis definition. (Terwilliger & Abdul-Hay, 2017) (Nunes et al., 2017) (Conter et al., 2010) In Italy, the current polychemotherapeutic protocol used for first onset Philadelphia negative ALL is the European AIEOP-BFM (Associazione Italiana di Ematologia ed Oncologia Pediatrica- Berlin-Frankfurt-Munster) 2017 protocol (ClinicalTrials.gov identifiers: NCT03643276, http://clinicaltrials.gov): this clinical trial investigates the benefit of the administration of innovative drugs, such as blinatumomab and the proteasomal inhibitor bortezumib, to the conventional chemotherapeutic agents. (Queudeville & Ebinger, 2021) (Sin & Man, 2021) However, thiopurines remain backbone drugs, and are used throughout the different therapeutic phases of the protocol. In particular, mercaptopurine is administered during the induction phases combined with other chemotherapeutic agents and during both consolidation and maintenance phases in combination with methotrexate, an antimetabolite of folic acid that inhibits different enzymes of the folate pathway, such as dihydrofolate reductase and thymidylate synthase, thus compromising DNA synthesis and inducing apoptosis. (Stocco et al., 2013) (Mikkelsen et al., 2011)

For IBD treatment, the therapeutic protocol includes two main phases: the first one consists in the induction of remission and the second one consists in the maintenance of remission. The therapeutic scheme for IBD includes the administration of immunomodulators, such as glucocorticoids, thiopurines and methotrexate, and also biologic drugs, such as infliximab. (van Hoeve & Vermeire, 2020) Thiopurines are administered to IBD pediatric patients accordingly to the European Crohn's and Colitis Organization (ECCO) and the Paediatric IBD Porto group of European Society of Paediatric Gastroenterology, Hepatology and Nutrition (ESPGHAN) guidelines. (Ruemmele et al., 2014) In particular, these immunomodulators are recommended for the remission and maintenance phases in pediatric patients presenting corticosteroid-dependence or with frequent relapse episodes. (Turner et al., 2018) In particular, thiopurines (2.0 – 2.5 mg/kg/day azathioprine or 1.0 – 1.5 mg/kg/day mercaptopurine) are recommended to maintain the steroid-free remission. (Riello et al., 2011)

## 1.2 Pharmacodynamics

Thiopurines are metabolized through a complex pathway into the active metabolites, responsible for drug efficacy. These metabolites are thionucleotides (TGN) that include thioguanosine mono-, di-, tri-phosphate (TGMP, TGDP, TGTP) and deoxythioguanosine mono-, di-, tri-phosphate (dTGMP, dTGDP, dTGTP). Different enzymes perform the conversion of mercaptopurine into TGN (Figure 2). In particular, hypoxanthine phosphoribosyltransferase 1 (HPRT1) is a transferase enzyme that catalyzes mercaptopurine conversion into thioinosine monophosphate (TIMP), inositol monophosphate dehydrogenase (IMPDH) is an oxidoreductase that catalyzes the conversion of TIMP into thioxanthosine monophosphate (TXMP) and guanosine monophosphate synthetase (GMPS) is a synthetase that converts TXMP into TGMP. Another important enzyme involved in the thiopurine biotransformation is inosine triphosphate pyrophosphatase (ITPA), a phosphatase responsible for the conversion of thioinosine triphosphate (TITP) to TIMP, which is a useful substrate for TGN synthesis. Thioguanine is directly converted into dTGMP/ TGMP by HPRT1 in a single step reaction. (Zaza et al., 2010) Like purine analogues, TGN exert their mechanism of action through different mechanisms: the TGN incorporation into nucleic acids and the blockage of *de novo* synthesis of purines, impairing the incorporation of canonical dGTP and GTP into DNA and RNA and subsequently inducing cell-cycle arrest and apoptosis. (Cara et al., 2004) Furthermore, Tiede and collaborators identified an additional cytotoxic mechanism of action exerted by thiopurines in T lymphoid cells, based on TGTP-mediated inhibition of the Ras-related C3 botulinum toxin substrate 1 (Rac-1), a GTPase of the Rho family, whose inactivation leads to apoptosis. (Tiede et al., 2003) Moreover, it has been recently hypothesized that these drugs could also affect autophagy, a biological process that plays a crucial role in cell fate regulation after environmental stress exposure. Interestingly, Chaabane and collaborators showed a potential interconnection between autophagy and apoptosis induced by thiopurines. In particular, they found increased autophagy levels after thiopurine exposure in different colorectal cancer cell lines, leading to the hypothesis that autophagy induction could be a cell protective mechanism against thiopurine-induced apoptosis and that its inhibition can promote cell death. Furthermore, their results suggest that thiopurines could be able to disrupt mitochondrial function, leading to the loss of mitochondrial transmembrane potential that is a key step for apoptosis induction. However, further investigations are needed to clarify these mechanisms. (Chaabane & Appell, 2016)

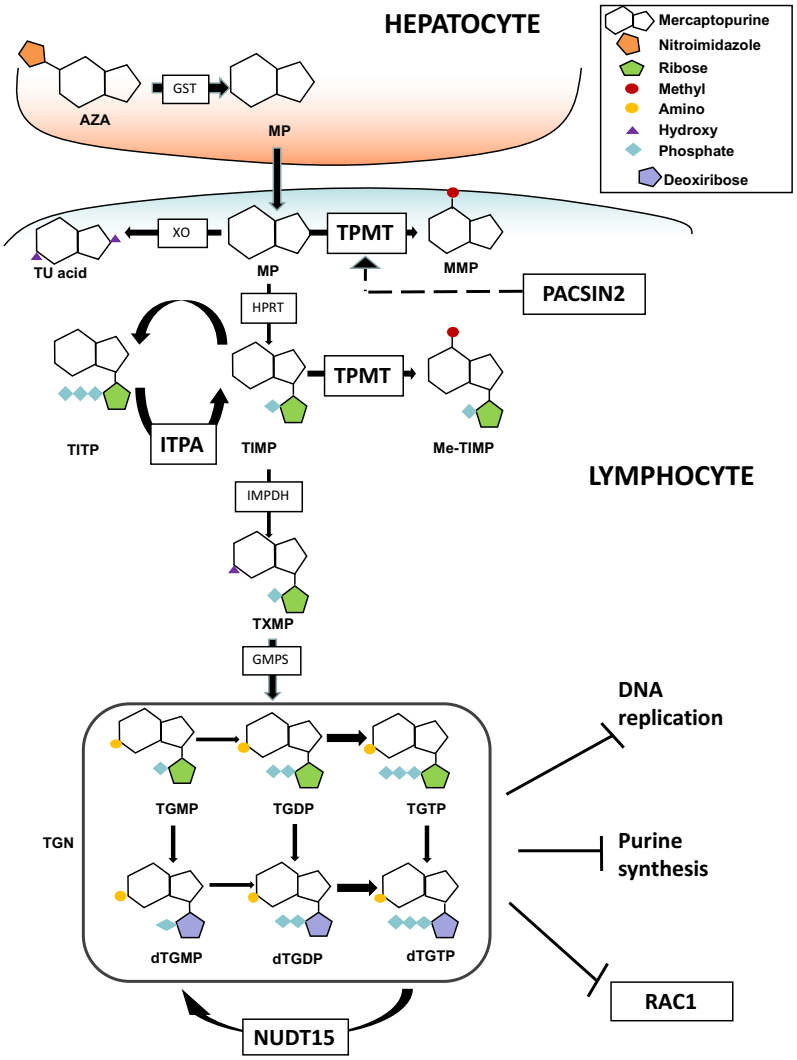


***Figure 2: Thiopurines pathway.*** *AZA: azathioprine, GMPS: GMP synthase, GST: glutathione-S-transferase, IMPDH: inosine monophosphate dehydrogenase, ITPA: inosine triphosphate pyrophosphatase, Me-TIMP: methyl-thioinosine monophosphate, Me-TITP: methyl- thioinosinetriphosphate, MP: mercaptopurine, MMP: methyl-mercaptopurine, NUDT15: nucleotide triphosphate diphosphatase gene, PACSIN2:Protein kinase C and casein kinase substrate in neurons protein 2, TGDP: thioguanine diphosphate, TGMP: thioguanine monophosphate, TGTP: thioguanine triphosphate, TIMP: thioinosine monophosphate, TITP: thioinosine triphosphate, TPMT: thiopurine methyltransferase, TGN: thioguanine nucleotide, TXMP: thioxantine monophosphate, TU acid: thiouric acid, XO: xanthine oxidase. (Franca et al., 2019)*

## 1.3 Pharmacokinetics

Thiopurines present a low bioavailability because they are rapidly metabolized by catabolic processes, mediated by xanthine oxidase (XO) and thiopurine methyltransferase (TPMT). In particular, XO is an oxidoreductase expressed in the liver and intestinal mucosa that catalyzes the conversion of mercaptopurine into thiouric acid, an inactive metabolite excreted in urine and TPMT is a ubiquitous transferase responsible for the conversion of mercaptopurine into methyl-mercaptopurine (MMP). MMP synthesis is in competition with the anabolic pathway of thiopurines. TPMT also catalyzes the S-methylation of different intermediates of TGN synthesis, producing secondary methylated nucleotides (MMPN), presenting potential cytotoxic activity through the inhibition of *de novo* purine synthesis. Indeed, the balance between TGN and MMPN levels is associated with both thiopurine clinical response and toxicity. (Adam de Beaumais et al., 2011) Thiopurine plasma concentration decreases rapidly after their oral administration, whereas the active metabolites persist for a long time in the blood; in particular, the serum peak of mercaptopurine is reached within 2 hours of drug administration and the half-life ranges from 20 to 120 minutes. In IBD, the clinical response to these antimetabolites is reached between weeks 8 and 17 of treatment. (Derijks et al., 2018) Despite of white blood cells being the molecular target of thiopurines, TGN are usually detected in red blood cells (RBC) by the third day of treatment and reach the steady state around the third week of treatment. (Karim et al., 2013) In IBD, TGN concentrations between 230 and 450 pmol/8 × $10^8$ RBC have been associated with clinical efficacy, whereas higher TGN concentrations have been related to a higher risk of myelosuppression and other complications, such as infections development. (Nguyen et al., 2011) Moreover, MMPN concentrations above 5700 pmol/8 × $10^8$ RBC were related to a higher hepatotoxicity risk in IBD pediatric patients. (Dubinsky et al., 2000) (Ruemmele et al., 2014) For ALL, some clinical protocols suggest mercaptopurine dose adjustment in case of TGN concentration above 1000 pmol/8 × $10^8$ RBC in order to avoid severe adverse reactions. (Lancaster et al., 2002) (Choi et al., 2021) Although the amount of TGN in RBC is commonly used as marker to determine thiopurine therapeutic efficacy and toxicity, TGN levels in RBC are not completely representative of the pharmacodynamic effects in leucocytes. Interestingly, it has been found that the RBC-TGN range is higher in patients treated with thioguanine compared to subjects exposed to mercaptopurine, because thioguanine undergoes a more rapid and more direct biotransformation. (Erb et al., 1998) While TGN values measured in RBC after thiopurines treatment should be interpreted with caution, the TGN concentration in the DNA could be

considered a possible biomarker for the therapeutic drug monitoring of thiopurines. (Franca, Braidotti, et al., 2021)

## 1.4 Adverse reactions

The most frequent adverse reaction of thiopurines treatment is the dose-dependent haematological toxicity that consist in neutropenia and leukopenia. (Gisbert & Gomollón, 2008) (Broekman et al., 2017) In addition, 5 to 20% of patients develop gastrointestinal (GI) toxicity with nausea, vomiting, stomatitis, abdominal pain or cramps, gastritis, stomach ulcer, GI bleeding, and diarrhea. (Sousa et al., 2020) Thiopurine treatment could be also associated with hepatotoxicity, pancreatitis, neurological complications and skin rashes. (Toksvang et al., 2019) (Ledder et al., 2015) (Tominaga et al., 2020)

## 1.5 Pharmacogenetics

Thiopurine pharmacogenetics has been deeply studied in the last decades, leading to important results for therapy personalization and underling the relevance of precision medicine. Nowadays, guidelines for thiopurine dosage adjustment based on patient's genotype have been provided; before starting thiopurine treatment, patients should be genotyped for genetic variants of clinical relevance, permitting the first-dose adjustment. (Relling et al., 2019) (Suarez-Kurtz et al., 2020) (Whirl-Carrillo et al., 2012) *TPMT* is considered the most important gene involved in thiopurine pharmacogenetics in Caucasians; the most frequent single nucleotide polymorphisms (SNPs) in Caucasians are rs1800462 (c.238G>C, p.Ala80Pro *TPMT*2*), rs1142345 (c.719A>G, p.Tyr240Cys, *TPMT*3C*), rs1800460 (c.460G>A, p.Ala154Thr, *TPMT*3B*) and the combination of rs1142345 and rs1800460, that constitute the *TPMT*3A* haplotype. *TPMT* homozygous variant allele carriers present a lower TPMT enzymatic activity, resulting in TGN accumulation and consequent increased risk of thiopurine-related toxicities. Heterozygous patients presenting an intermediate enzymatic activity are approximately 5–11% of Caucasians, whereas a homozygous variant genotype for *TPMT* is associated with a null or very low enzyme activity and it is detectable approximately in 1 to 300 Caucasian individuals, who are considered poor metabolizers. (Yates et al., 1997) (Franca et al., 2019) Interestingly, only the *TPMT**3A and the *TPMT**3C variants have been reported in African populations. (Adehin & Bolaji, 2018)

Another relevant gene for thiopurine pharmacogenetics is *NUDT15*, which encodes for a hydrolase that dephosphorylates the active metabolites TGTP and dTGTP into the inactive TGMP and dTGMP, preventing TGTP and dTGTP incorporation into the DNA. An altered NUDT15 enzyme activity has been associated with higher risk of thiopurine adverse reactions, such as myelosuppression. (Khaeso et al., 2021) *NUDT15* could present many variant alleles. The most frequent *NUDT15* polymorphisms associated with an altered NUDT15 enzyme activity and with thiopurine adverse reactions are rs116855232 (c.415C>T, p.Arg139Cys), rs147390019 (c.416G>A, p.Arg139His), rs186364861 (c.52G>A, p.Val18Ile) and rs746071566 (36_37insGGAGTC, p.Val18_Val19insGlyVal). (Moriyama et al., 2016) (Suiter et al., 2020) These variants are more common in East Asians and Hispanics, while they are rare in Caucasians and not detectable in Africans; thus, *NUDT15* polymorphisms are considered useful pharmacogenetic markers to adjust drug dosage before treatment beginning in these populations, where the prevalence of *TPMT* variants is very rare. (Relling et al., 2019)

## 1.6 Other possible biomarkers of thiopurines response

Although *TPMT* genotyping has improved thiopurine dose adjustment, reducing the risk of drug related adverse reactions, there are *TPMT* wild type patients who present toxicity during therapy with thiopurines. Despite different genome-wide studies performed on ALL pediatric patients with thiopurine toxicities identified the TPMT enzyme activity as a monogenic trait, it has been hypothesized that other factors could affect thiopurine response. (Franca, Zudeh, et al., 2021) An agnostic study performed on human HapMap cell lines identified the protein kinase C and casein kinase substrate in neurons 2 (*PACSIN2*) as the main TPMT trans-acting gene, whose expression and SNP rs2413739 (C>T) impact significantly on TPMT activity (Figure 3). (Stocco et al., 2012)

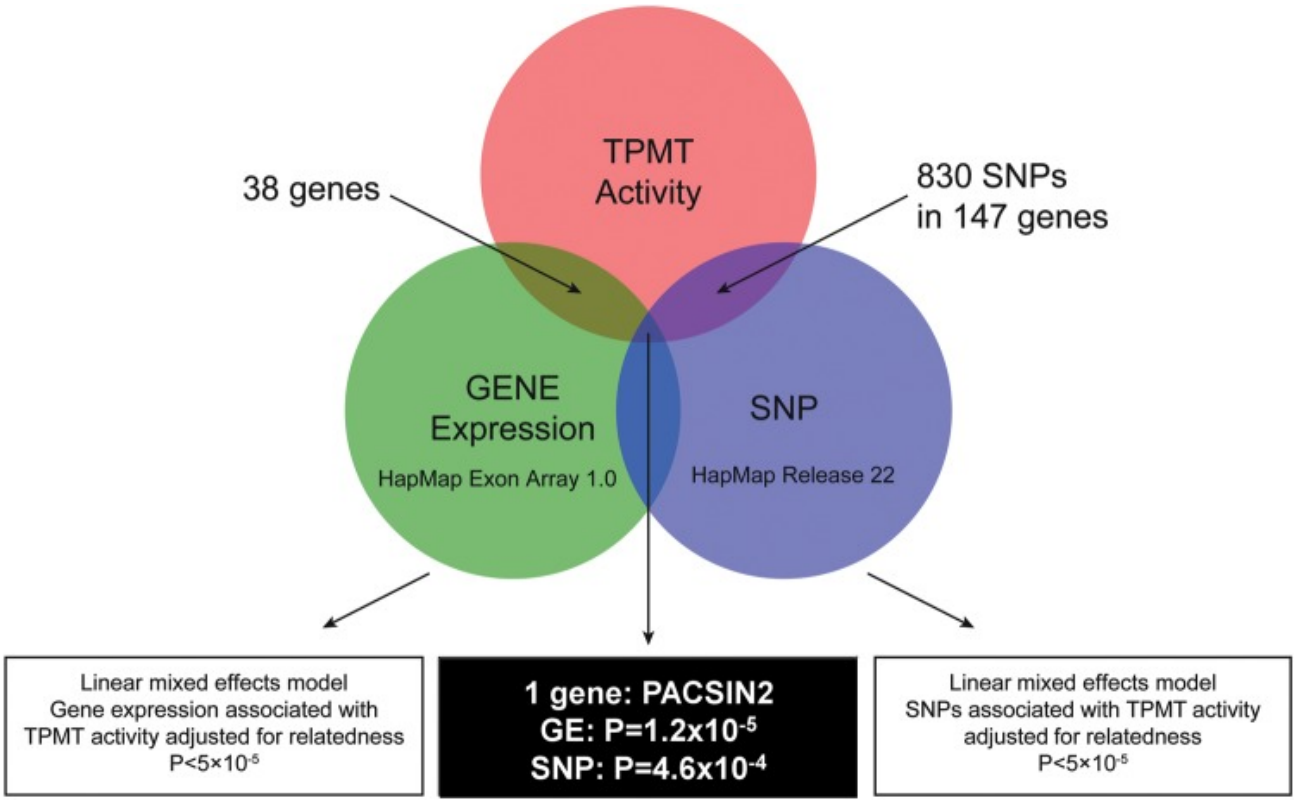


***Figure 3: Diagram describing the analysis strategy used by Stocco and collaborators to identify the most important genes whose expression and SNPs are associated with TPMT activity in a cohort of HapMap cells****. Among the genes whose expression was highly associated with TPMT activity, PACSIN2 was the only one presenting a SNPs significantly associated with TPMT activity (P-value <0.0005). (Stocco et al., 2012)*

*PACSIN2* rs2413739 is a non-coding variant located in an expression quantitative trait loci (eQTL) region of *PACSIN2*. It was significantly associated with reduced TPMT activity and also with a higher risk of severe thiopurine related GI toxicity in two independent cohorts of ALL pediatric patients, exposed to mercaptopurine during the consolidation phase according to the Saint Jude Children's Research Hospital (SJCRH) Total 13B protocol and the AIEOP-BFM 2000 protocol, respectively. (Stocco et al., 2012) These results were further validated in another independent cohort of Italian ALL pediatric patients, treated according to the AIEOP-BFM ALL 2009 protocol. (Franca et al., 2020) This study evaluated also the possible impact of this SNP on thiopurine response in a group of IBD pediatric patients: no significant effect of *PACSIN2* rs2413739 on TPMT activity was observed, however, authors found a reduced azathioprine effectiveness in IBD pediatric patients carrying the T variant allele. (Franca et al., 2020) A retrospective Slovenian study performed on ALL pediatric patients undergoing thiopurine therapy according to different protocols, such as the Pediatric Oncology Group (POG) and BFM -83, −86, −90, −95 and IC2002, found the *PACSIN2* polymorphism as a significant risk factor for the development of thiopurine-related haematological toxicity in wild type *TPMT* patients during the

maintenance phase of therapy. (Smid et al., 2016) Furthermore, a recent study performed on ALL pediatric Korean patients showed an association between the TT genotype of *PACSIN2* rs2413739 and mercaptopurine biotransformation level (TGN/mercaptopurine dose ratio). (Choi et al., 2019)

# 2. PACSIN2

PACSIN2 is a member of the PACSIN family of proteins, which are intracellular adapter proteins involved in vesicle transport, membrane dynamics and actin reorganization. (Grimm-Günter et al., 2008) There are 3 PACSIN isoforms: PACSIN1, PACSIN2 and PACSIN3. In particular, PACSIN1 is specifically expressed in the neural tissues, whereas PACSIN3 is expressed in skeletal muscle and heart; PACSIN2 is ubiquitous. PACSIN2 plays a role in the regulation of endocytosis and in the morphogenesis and formation of caveole, which are small invaginations of the plasma membrane involved in receptor-independent endocytosis. These structures are also involved in other biological processes, such as the pathogens entry into cells and tumorigenesis. All three PACSIN isoforms contain an N-terminal F-BAR domain and a C-terminal SH3 domain. (Figure 4) (Senju et al., 2011)

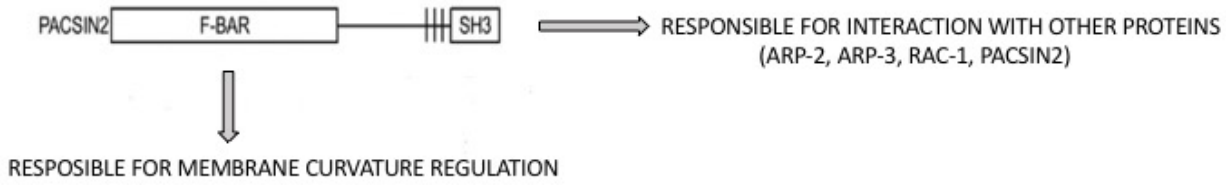


***Figure 4: schematic representation of the PACSIN2 protein domains.*** *The N-terminal F-BAR domain of PACSIN2 is responsible for PACSIN2 association to cell membrane and plays a key role in membranes curvatures, tabulation and invaginations during different biologic processes. The C-terminal SH3 domain of PACSIN2 is important for the physical binding to other proteins permitting the regulation of different processes, such as cell spreading and migration.*

The N-terminal F-BAR domain of PACSIN2 regulates membrane curvatures, tubulation, and invagination during the vesicle budding process, endocytosis and caveole biogenesis. (Senju et al., 2015) SH3 C-terminal domain mediates the interaction with many different membrane proteins. The SH3 domain of PACSIN2 can bind the proline-rich (PRD) domain of dynamin 2, suggesting a possible link between caveolae and dynamin-2-mediated membrane scission (Daumke et al., 2014) PACSIN2 C-terminal can also bind Arp2/3, an activator of N-WASP,

stimulating actin polymerization. (Kessels & Qualmann, 2002) Moreover, Rhao and collaborators identified an intramolecular interaction between the F-BAR and SH3 domains of PACSIN2, suggesting an auto-inhibitory function of PACSIN2 with a consequent impaired membrane binding activity. (Rao et al., 2010) Finally, several evidences showed a possible interaction between PACSIN2 and Rac-1, an important protein involved in cell spreading and migration. (de Kreuk et al., 2011) Interestingly, Rac-1 plays also a role in thiopurine mechanism of action: the thiopurine metabolite TGTP, a competitive antagonist of GTP, is able to bind Rac-1 and suppress its activation, stimulating apoptosis. Taken together, these evidences suggest that PACSIN2, Rac-1 and their expression levels could be considered for their role in thiopurine response, and that it would be interesting to investigate their function. (Franca et al., 2020) (Seinen et al., 2016)

Interestingly, an *in vitro* analysis performed on the NALM6 B-lineage ALL human cell line presenting the stable *PACSIN2* knock-down (KD) showed a reduction in both TPMT mRNA expression level and TPMT enzyme activity; then, thanks to an agnostic approach, authors showed that autophagy was among the main pathways affected by the *PACSIN2* KD. (Stocco et al., 2012) Moreover, PACSIN1 is involved in autophagy regulation, decreasing both the mechanistic target of rapamycin complex 1 (mTORC1) phosphorylation and activity levels. (Szyniarowski et al., 2011)

# 3. Autophagy

Autophagy is derived from Greek words that literally mean ‘self-eating’ and indicate a lysosome-dependent degradative mechanism of cytosolic material. It is used by eukaryotic cells to eliminate a source of stress or damage, like misfolded proteins, old organelles and intracellular bacteria; autophagy is also used to produce energy after nutrient deprivation. (Chun & Kim, 2018) Degradation products obtained from this process are transported across the lysosomal membrane into the cytoplasm, where they are recycled to produce proteins and ATP. (Yorimitsu & Klionsky, 2005) Autophagy encompasses three main catabolic pathways (i.e., macroautophagy, chaperone-mediated autophagy and microautophagy) that mediate lysosomal degradation of intracellular cargoes in order to maintain cellular homeostasis. Macroautophagy (hereafter referred as autophagy) is the most studied and it is suited for the degradation of large cargoes, like intracellular bacteria and protein aggregates. It consists in the generation of a membrane phagofore from a region of the endoplasmic reticulum (ER), which is followed by its elongation

and maturation to create an autophagosome that will be fused to lysosomes. (Figure 5) (Zhao & Zhang, 2019)

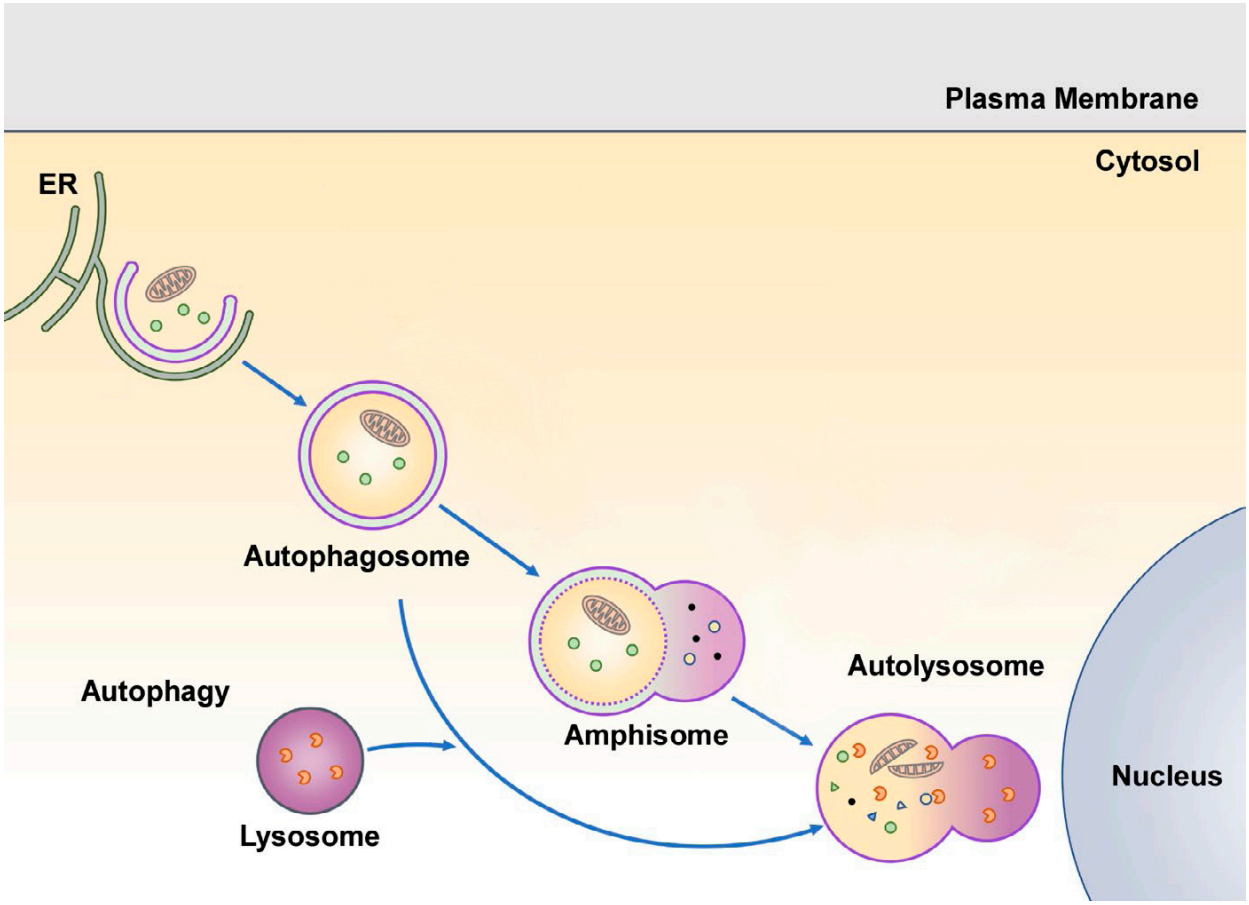


***Figure 5: schematic representation of autophagy.*** *The autophagosome derives from ER membrane and, after elongation and maturation phases, it is fused with lysosomes in order to degrade its cargoes. (Zhao & Zhang, 2019)*

The chaperone-mediated autophagy consists in the transport of cytosolic proteins though a specific target recognition performed by the chaperone protein HSC70 that is followed by the fusion with lysosomes thanks to the lysosomal LAMP-2A protein. (Kaushik & Cuervo, 2012) Finally, the microautophagy consists in an extension and engulfment of part of the lysosomal membrane to enwrap a small portion of the cytoplasm to incorporate proteins or organelles. (Oku & Sakai, 2018)

Autophagy could also be classified as selective and non-selective; in the nonselective autophagy the phagophore is not connected to any specific cargo, enabling a random engulfment of cytoplasmic material, whereas in the selective autophagy the cargo is linked to the growing phagofore thanks to specific receptors and molecular complexes, to degrade a specific target

molecule in the cytoplasm. (Figure 6) (Lamark et al., 2017) Recently, many different types of selective autophagy have been identified, such as such as mitophagy (selective degradation of mitochondria), pexophagy (selective degradation of peroxisomes), the piecemeal microautophagy of the nucleus, ribophagy (ribosomal degradation), and lipophagy, an alternative pathway of lipid degradation mediated by lysosomal hydrolases. (Gubas & Dikic, 2022)

## 3.1 Autophagy machinery

Autophagy consists in a series of sequential events that permit the engulfment of different cytoplasmic cargoes in a double-membrane autophagosome and their delivery for degradation. The molecular mechanisms at the basis of this process were discovered in yeast, identifying autophagy-related (ATG) genes which play a crucial role in every phase of this pathway. During autophagosome biogenesis, the ATG proteins form different complexes and act coordinately. (Zhao & Zhang, 2019) In particular, the ATG1 complex (composed by ATG1, ATG13, and ATG17 proteins) and phosphatidylinositol 3-phosphate (PI(3)P) kinase complex (composed of VPS34, VPS15, ATG6/Beclin1, and ATG14 proteins) are required for nucleation of the inner membrane (IM) of the phagofore. IM is a cup-shaped autophagosomal precursor structure derived from a specific region of ER, called omegasome, that is particularly enriched in PI(3)P. The presence of the integral membrane proteins ATG9 are important in the IM initiation; however, the ATG9 proteins are then removed from autophagosomal membranes, thanks to a process controlled by the ATG2/ATG18 complex. Finally, two ubiquitin-like conjugation systems, including ATG7 (E1 enzyme)/ATG3 (E2 enzyme)/Atg8 family members (ubiquitin-like molecules) and ATG7/ATG10 (E2 enzyme)/ATG12 (ubiquitin-like molecule) are involved in autophagosomal membrane expansion and closure. Finally, in yeast, the autophagosome digestion occurs in the vacuole. (Nakatogawa et al., 2009)

In multicellular eukaryotic organisms, autophagy consists in a more complex pathway, presenting additional stages. (Zhao & Zhang, 2019) Upon autophagy induction, the ULK1/FIP200 complex (the mammalian orthologous ATG1 complex) is targeted to the ER in order to recruit the PI(3)P kinase complex for the generation of omegasomes, that are considered the starting platforms for IM nucleation and expansion. In multicellular organisms, membrane sources for the nucleation of IMs may include COPII vesicles, ATG9 vesicles and also the plasma membrane, mitochondria and the ER–Golgi intermediate compartment (Lamb et al., 2013) (Karanasios et al., 2016) (Zhao & Zhang, 2019). In particular, the ULK1/FIP200 complex binds the ER-resident tail-anchored

VAP proteins (VAPA and VAPB) to stabilize the ULK1/FIP200 complex at the autophagosome formation sites on the ER. Then, the ER-transmembrane protein EPG-3/VMP1 will be disassembled from the ER–IM contacts, stimulating the final IM closure into autophagosomes. This process is mediated by the endosomal sorting complex required for transport (ESCRT) and also by the ATG8 conjugation system; during this phase a change in morphology of the neo-synthetized phagofore from an elliptical expanding IM to spherical sealed autophagosomes occurs. (Zhao & Zhang, 2019) The neo-synthetized autophagosomes show a double-membrane structure, but their structure change during maturation leading to the formation of amphisomes, a single limiting membrane vesicle that is ready to be fused with lysosome to generate autolysosomes. In some cases, after autophagosomes formation and maturation, these vesicles may be fused to endosome deriving from the endocytic pathway. (Tooze et al., 1990) (Chun & Kim, 2018) For the mature autophagosomes fusion with lysosomes two multiprotein SNARE complexes play a crucial role, promoting an efficient fusion between autophagosomes and lysosomes; in particular, one is composed by the autophagosomal-localized STX17, SNAP29 and the endolysosomal-localized VAMP8/VAMP7 proteins, whereas the other one is formed by autophagosomal -SNARE YKT6, SNAP29 proteins and the lysosomal-localized SNARE STX7 protein. (Abada et al., 2017) Also the lysosomal protein LAMP2 promotes fusion of lysosomes with autophagosomes/amphisomes. (Eskelinen et al., 2002) After autolysosome formation, these vesicles move along microtubules from the center to the periphery of the cells and it was reported that their presence in the peripheral regions of the cytoplasm affects the activity mTORC1, that is a considered the epicenter of the cellular nutrient sensing. (Rabanal-Ruiz et al., 2017) When nutrients are available, mTORC1 promotes cell growth by stimulating different biosynthetic pathways, such as synthesis of proteins, lipids and nucleotides and by blocking autophagy, negatively regulating the ULK1/FIP200 complex. After starvation or stress conditions, mTORC1 is inactivated, promoting autophagy. (Rabanal-Ruiz et al., 2017) In addition, the release of amino acids in the cytoplasm after the autolysosomes digestion, mediated by the proton-assisted amino acid transporter (PAT) 1, inhibits mTORC1 activation. (Zoncu et al., 2011)

## 3.2 Autophagy markers

In yeast, ATG8 family proteins are involved in different stages of autophagy, such as autophagosomes formation, elongation and maturation. (Schaaf et al., 2016) In higher eukaryotes the ATG8 proteins has six ATG8 homologues, classified in the LC3 subfamily (LC3A, LC3B, and LC3C) and in the GABARAP subfamily (GABARAP, GABARAPL1, and GABARAPL2). The LC3 subfamily promotes elongation of the phagofore, while the GABARAP subfamily is involved in the step of autophagosome closure; LC3B (hereafter referred to as LC3, also called MAP1LC3B (Microtubule associated protein 1B light chain 3B)) is one of the most studied autophagic proteins because it is fundamental for autophagosome development, elongation and closure. (Zhao & Zhang, 2019) LC3 is present in the cytoplasm at basal level in the form LC3-I, and is conjugated to phosphatidylethanolamine (PE) to form LC3-II after autophagy induction. LC3 lipidation is required for LC3 attachment to both the inner and outer membrane of the expanding phagophore and it plays a crucial role for it elongation, maturation and closure. (Tanida et al., 2008) The amount of LC3-II reflects the number of autophagosomes and structures linked to autophagy and is a gold standard marker of autophagy. (Klionsky et al., 2021) The increase in LC3-II is associated not only with the activation of autophagy, but also with the inhibition of autophagosome degradation. (Yoshii & Mizushima, 2017) Another widely studied protein to monitor autophagy in eukaryotic cells is the sequestosome-1 (SQSTM1/P62) receptor. SQSTM1/P62 consists of 440 amino acids and contains a Phox-BEM1 (PB1) domain at the N-terminal, that allows polymerization of the protein, a ZZ-zinc-finger domain, a nuclear localization signal (NLS), an export motif (NES), an LC3-interacting region (LIR), a Keap1-interacting region (KIR) domain and an Ubiquitin-associated (UBA) domain at the C-terminus, capable of binding the ubiquitin tag present on cytoplasmic molecules ready to be degraded. (Birgisdottir et al., 2013) Around 30% of synthesized proteins in cells are misfolded under normal conditions and are ubiquitinated by the ubiquitin–proteasome system (UPS) that plays a fundamental role in the degradation of these proteins. (Grumati & Dikic, 2018) Ubiquitinated proteins non-covalently interact with the UBA domain of SQSTM1/P62, which binds also LC3-II thanks to a LIR domain, permitting the elongation of the neo-synthetized phagofore selectively around the ubiquitinated cargo. (Myeku & Figueiredo-Pereira, 2011) This mechanism leads to the inclusion of SQSTM1/p62 inside the neo-autophagosome that will be digested by lysosomes. (Liu et al., 2016) Thus, the lower amount of SQSTM1/P62 is considered a marker of the autophagic activity. (Klionsky et al., 2021) (Figure 6)

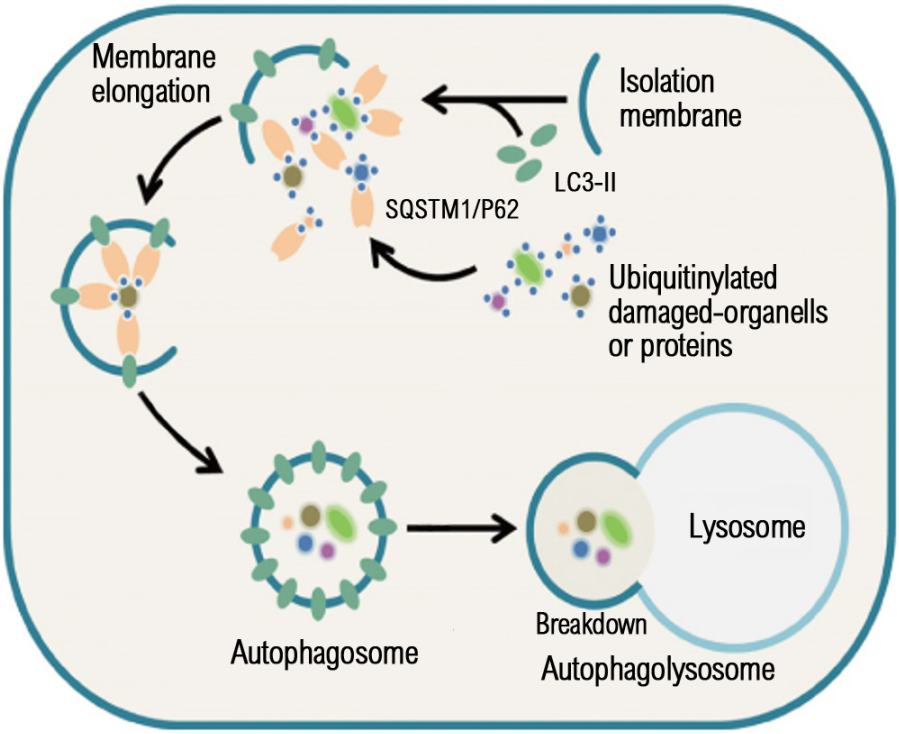


***Figure 6: schematic representation of LC3-II and SQSTM1/P62 role in autophagy.*** *Both LC3-II and SQSTM1/P62 are involved in the first phases of the autophagic flux; LC3-II mediates autophagosomes elongation and maturation, whereas SQSTM1/P62 mediates receptor-mediated autophagy, thanks to a physical binding with LC3 and ubiquitinated cargoes that are targeted for autophagy degradation. (S. I. Kim et al., 2019)*

## 3.3 LIR domain

Many autophagy proteins, such as the cargo receptor SQSTM1/P62, involved in different stages of autophagy, present an evolutionarily conserved LIR motif in their amino acid sequence, indicating a crucial role of LC3 during many phases of the autophagy machinery, such as autophagosomes formation and maturation. (Birgisdottir et al., 2013) The canonical LIR motif is a small domain presenting the consensus amino acid core sequence [W/F/Y]xx[L/I/V], where "x" is any amino acid. The presence of an aromatic amino acid and an aliphatic residue in the LIR motif is fundamental for the protein interaction with the hydrophobic pocket 1 (HP1) and HP2 of the LIR docking site in LC3. (Wirth et al., 2019) Most LIR motifs show W or F at the aromatic position, and only a few have Y at this position; structural data on *NRB1* gene showed that the presence of W in the LIR motif core confers a greater binding affinity to LC3 than F or Y. (Rozenknop et al., 2011) Electrostatic interactions should determine the substrate specificity of the ATG8 homologs, such as LC3. Interestingly, the F-type LIR motifs may have a preference for the GABARAP subfamily proteins. (Alemu et al., 2012)

Jacomin and collaborators developed a freely available web database, called iLIR (https://ilir.warwick.ac.uk) to identify LIR-containing proteins in 8 different model organisms. Thanks to this *in silico* system, authors redefined the LIR motif consensus sequence as: (ADEFGLPRSK)(DEGMSTV)(**WFY**)(DEILQTV)(ADEFHIKLMPSTV)(**ILV**), where the residues marked in bold in the third and in the last position correspond to the most important residues required for the interaction with ATG8-family proteins. (Jacomin et al., 2016)

# 4. Apoptosis

Apoptosis is a eukaryotic mechanism of programmed cell death that occurs normally during aging and plays a role in the maintenance of tissue homoeostasis. This type of cell death consists in cells dismantling, thanks to the production of membrane-enclosed vesicles that are engulfed by phagocytes, thus preventing the release of intracellular components into the surrounding tissue. (Edinger & Thompson, 2004) Apoptosis is stimulated by different stress conditions, such as the exposure to drugs and chemical agents able to induce a DNA damage. Moreover, the exposure to some hormones, such as corticosteroids, may lead to apoptosis in some cell types (e.g., thymocytes) but not in others, whereas other cells are unaffected or even stimulated by the same molecules. (Elmore, 2007) The apoptotic process is morphologically characterized by a cell shrinkage, followed by the chromatin condensation and the formation of apoptotic bodies during a process called "blebbing". (Elmore, 2007) Biochemically, these processes are associated with the energy-dependent activation of the cysteine proteases "caspase" cascade. (Harvey & Kumar, 1998) Depending on the origin of the stimulus (intrinsic or extrinsic signals), apoptosis is executed through the activation of either the extrinsic (receptor mediated) pathway or the intrinsic (mitochondrial mediated) pathway. Different extracellular or intracellular stimuli lead to the activation of the downstream effector caspase-3 that migrates into the nucleus leading to endonucleases activation, DNA degradation, proteases activation and cytoskeletal reorganization. (Borutaite, 2010) In particular, the presence of different intracellular stimuli, such as hypoxia, stimulates the disruption of the outer mitochondrial membrane, leading to the release in the cytoplasm of pro-apoptotic factors, including cytochrome c, from the mitochondrial intermembrane space. (Borutaite, 2010) Cytochrome c interacts with the apoptotic protease-activating factor-1 (APAF-1) and stimulates the APAF-1 ATP-dependent oligomerization, leading to the generation of a caspase-activating complex called "Apaf-1 apoptosome", that recruits and activates the casapase-9 that in turn activates the effector caspase-3. (Bratton &

Salvesen, 2010) Similarly, the binding of death ligands, toxins or cytotoxic T cells to death receptors on the plasma-membrane, leads to the activation of an apical caspase (i.e., caspase-8 or caspase-9), which in turn activates the downstream effector caspases-3 and caspase-7. Caspase-3 migrates into the nucleus and cleaves different substrates, such as the poly-adenosine diphosphate-ribose polymerase-1 (PARP1), various cytokeratins, the plasma membrane cytoskeletal protein Alpha Fodrin, the nuclear protein NuMA and the endonuclease CAD, responsible of DNA fragmentation and chromatin condensation. (Elmore, 2007) Caspase-3 also induces cytoskeletal reorganization and disruption, promoting apoptotic bodies formation that are uptaken by phagocytes thanks to the externalization of phosphatidylserine on the surface of apoptotic bodies. (Figure 7) (Virág, 2005)

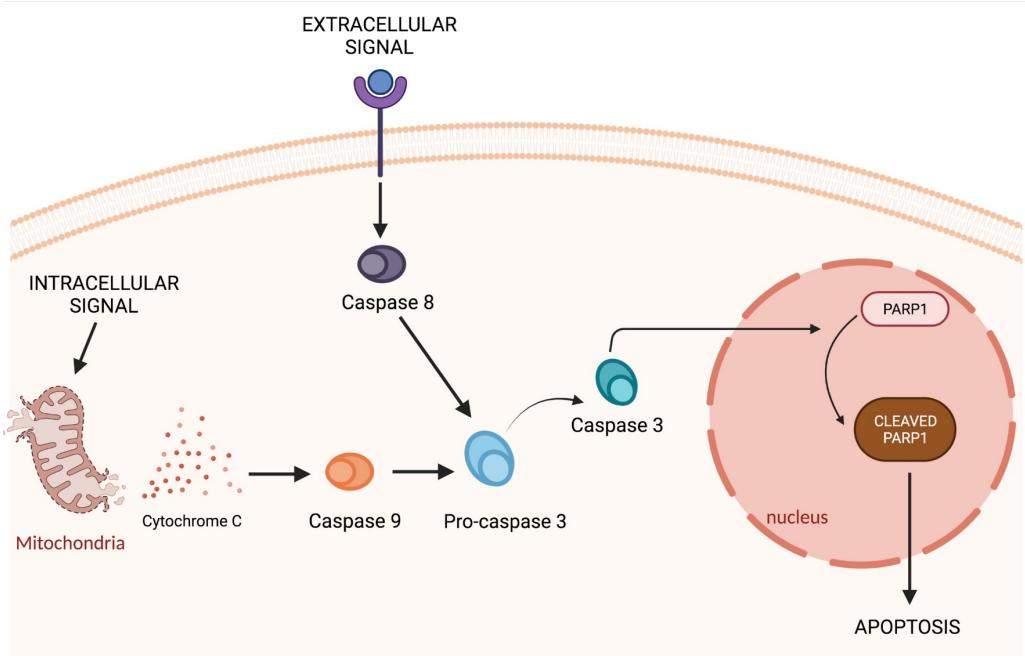


***Figure 7: Schematic representation of apoptosis.*** *Both intrinsic and extrinsic pathways led to caspase 3 activation, that mediates the cleavage of PARP1, stimulating apoptosis.*

## 4.1 PARP1

PARP1 is an enzyme of the PARP family of proteins, involved in DNA damage repair. Nowadays, at least 18 members of the PARP family have been characterized; however, PARP1 is the best-known isoform. After activation, PARP1 catalyzes ADP-ribose transfer from the nicotinamide adenine dinucleotide (NAD+) to many different nuclear proteins, such as histones, DNA polymerases and topoisomerases, transcription factors, and also to PARP1 itself, regulating a variety of physiologic processes. A massive activation of PARP1 leads to the activation of the intrinsic apoptosis. (Wang et al., 2011) The poly(ADP-ribosyl)ation is a protein post-translational modification that consists in the synthesis of ADP-ribose polymers on target proteins. Poly(ADP-ribosyl)ation occurs in all nucleated cells of higher eukaryotes. In the absence of DNA damage, the amount of poly(ADP-ribosyl)ated proteins is low, whereas after DNA single strand and double strand breaks, PARP1 is rapidly activated increasing poly(ADP-ribose) levels and facilitating DNA repair. (Bouchard et al., 2003) In case of mild DNA damage, the increase of poly(ADP-ribose) levels stimulates the recruitment of DNA repair proteins and nucleases to promote DNA repair; however, in presence of an excessive DNA damage, the massive activation of PARP1 consumes NAD+ and ATP reserves for poly(ADP-ribosyl)ation, leading to necrosis. During apoptosis, PARP1 is cleaved by caspase-3 into an ~25 kDa N-terminal fragment and an ~85-kDa C-terminal fragment, that retains enzymatic activity; this cleavage blocks PARP1 activation in response to DNA fragmentation, protecting the cells from ATP depletion and subsequent necrotic cell death. Indeed, the presence of the cleaved fragments of PARP1 are considered markers of apoptosis induction. (Kim et al., 2005)

PARP1 can be involved also in a caspase-independent apoptotic mechanism, associated to the apoptosis-inducing factor (AIF), a pro-apoptotic flavoprotein residing in the mitochondrial intermembrane space; AIF acts as trigger of apoptosis. After release in the cytoplasm, AIF migrates into the nucleus and induces peripheral chromatin condensation and DNA fragmentation. Interestingly, PARP1 inactivation by cleavage prevents its futile attempts of DNA repair, helping apoptosis. (Kim et al., 2005)

# AIM

Thiopurines are metabolized through a complex pathway in order to generate the active thiopurine metabolites. The methyltransferase TPMT is involved in the thiopurine catabolic pathway and reduced TPMT enzyme activity is associated with a higher risk of drug related adverse reactions development. (Relling et al., 2019) PACSIN2 is able to modulate TPMT activity through unknown molecular mechanisms. Moreover, the rs2413739 variant, present in an eQTL region of *PACSIN2*, was found to be associated with a reduced TPMT enzyme activity and has been also related to a higher risk of thiopurine-related GI toxicity in different independent cohorts of ALL pediatric patients and to a reduced azathioprine effectiveness in a group of IBD pediatric patients. (Stocco et al., 2012) (Franca et al., 2020)

PACSIN2 is a protein involved in endocytosis and caveole formation (de Kreuk et al., 2012) (Senju et al., 2011) and a previous agnostic analysis identified autophagy as the main pathway affected by *PACSIN2* KD in a human B lymphoid cell line. (Stocco et al., 2012)

This thesis aims to evaluate the possible role of PACSIN2 in autophagy and to investigate the possible impact of *PACSIN2* KD on mercaptopurine cytotoxicity and on TPMT levels in lymphoid and intestinal models. Furthermore, this project aims to evaluate the possible effect of both mercaptopurine exposure and *PACSIN2* KD on autophagy and apoptosis in an intestinal *in vitro* model.

# MATERIAL AND METHODS

## 1. Cell lines

Engineered cell lines presenting stable modifications were previously generated at the SJCRH (Stocco et al., 2012), and kindly provided by prof. W:E: Evans (SJCRH, Memphis, Tennessee, USA). In particular, a human peripheral blood leukemia pre-B cell line (NALM6) and a human colon adenocarcinoma cell lines (LS180) were transfected with a lentivirus encoding for a shRNA (GAACGATGACTTCGAGAAGAT) to determine the stable *PACSIN2* KD (KD cells); as control, cells were transfected with a lentivirus encoding for a control shRNA (MOCK cells). NALM6 MOCK and NALM6 KD were further transfected with a plasmid encoding for wild type *TPMT*1* (RC203309 Origene) to present the stable TPMT overexpression (NALM6*1 and NALM6 KD*1).
NALM6 and LS180 cell lines were grown in RPMI-1640 (ECB9006L Sigma-Aldrich) containing 10% FBS (F7524 Sigma-Aldrich), 20 mM glutamine (FCB3000D ThermoSCIENTIFIC) and 1% penicillin/streptomycin (P0781 Sigma-Aldrich) accordingly to standard procedures: 37 °C in presence of 5% $CO_2$.

## 2. Treatments

Treatment used to evaluate the impact of *PACSIN2* KD and TPMT*1 overexpression on autophagy and drug sensitivity in different cell lines are summarized in table 1.

| Cell line* | Treatment concentration range | Treatment duration (hours) | Aim | Assay | Figure |
|---|---|---|---|---|---|
| NALM6, LS180 | chloroquine (30 µM) | 4, 24 | to investigate the autophagic flux | immunoblotting | 10 |
| NALM6 | mercaptopurine (from 0.313 µM to 20 µM) | 72 | to evaluate drug sensitivity | MTT drug sensitivity assay | 14 |
| NALM6 | tunicamycin (from 0.0005 µM to 50 µM) | 72 | to evaluate unfolded protein stress response | MTT drug sensitivity assay | 14 |
| LS180 | mercaptopurine (from 0.313 µM to 160 µM) | 72 | to evaluate drug sensitivity | MTT drug sensitivity assay | 14 |
| LS180 | thioguanine (from 0.015 µM to 100 µM) | 72 | to evaluate drug sensitivity | MTT drug sensitivity assay | 14 |
| LS180 | fluorouracil (from 0.137 µM to 100 µM) | 72 | to evaluate drug sensitivity | MTT drug sensitivity assay | 14 |
| LS180 | tunicamycin (from 0.05 µM to 156 µM) | 72 | to evaluate unfolded protein stress response | MTT drug sensitivity assay | 14 |
| LS180 | mercaptopurine (1.25 µM and 2.5 µM) | 24, 48 | to evaluate autophagy induction | immunoblotting | 15 |
| LS180 | mercaptopurine (1.25 µM and 2.5 µM); doxorubicin (5 µM, positive control) | 24, 48 | to evaluate apoptosis induction | immunoblotting | 16 |
| LS180 | mercaptopurine (1.25 µM and 2.5 µM); doxorubicin (5 µM, positive control) | 24, 48, 72 | to evaluate mitochondrial membrane potential alterations | DiOC6 assay | 16 |
| LS180 | mercaptopurine (2.5 µM) | 24, 48 | to evaluate levels of thiopurines metabolites | HPLC-UV analysis | 17 |

***Table 1: treatments overview**. Treatments were performed on available engineered cells lines (NALM6 MOCK, NALM6 KD, NALM6*1, NALM6 KD*1, LS180 MOCK, LS180 KD). DiOC6: 3,3'-dihexyloxacarbocyanine iodide; HPLC-UV: High Performance UV Liquid Chromatography; MTT: 3-(4,5-Dimethylthiazol-2-yl)-2,5-Diphenyltetrazolium Bromide.*

The autophagic flux was investigated exposing cells to chloroquine, a substance that impairs autophagosomes fusion with lysosomes. (Yoshii & Mizushima, 2017) The effect of both *PACSIN2* KD and *TPMT*1* overexpression on unfolded protein response was investigated after tunicamycin exposure. (Park et al., 2016) For mercaptopurine, the effect of *PACSIN2* KD on cytotoxicity in LS180 cells was evaluated; moreover the induction of both autophagy and apoptosis after mercaptopurine treatment on LS180 cells with *PACSIN2* KD was investigated. The possible impact of *PACSIN2* KD on the purine analogue thioguanine and the antimetabolite fluorouracil was investigated in LS180

cell lines. For NALM6 cells, the impact of both *PACSIN2* KD and TPMT*1 overexpression on mercaptopurine sensitivity was investigated.

## 3. Patients' samples

Fifteen IBD pediatric patients were enrolled at the Gastroenterology unit of the Pediatric Department of the Institute for Maternal and Child Health IRCCS Burlo Garofolo in Trieste. Local ethical committee approval for the study was provided. The study was conducted in accordance with the principles outlined in the Declaration of Helsinki, and the parents of all the participating children gave written informed consent before study participation. For each patient, during the diagnostic colonoscopy, inflamed and non-inflamed tissues were collected in Trizol (product number 15596026, Thermo Scientific) for RNA isolation or in phosphate buffer saline (PBS) supplemented with Halt Protease Inhibitor Cocktail 1x (Catalogue number (#): 87786, Thermo Fisher Scientific) for protein lysates preparation.

## 4. Cell lysates preparation

Cells lines were pelleted by centrifugation at 600 xg for 5 minutes, washed once with PBS and suspended in lysis buffer (10 mM Tris-HCl pH 7.4, 0.1% SDS, 100 mM NaCl, 100 mM EDTA), supplemented with Halt™ Protease Inhibitor Cocktail 1x. Intestinal biopsies from 5 IBD pediatric patients of our cohort were lysed in RIPA buffer (89901, Thermo Fisher Scientific) supplemented with Halt™ Protease Inhibitor Cocktail 1x (78430, Thermo Fisher Scientific). After pellet incubation with lysis buffer, sonication was performed: 80% amplitude, 10 seconds ON, 30 seconds OFF. Then, after 10 minutes of centrifugation at 16000 per g and 4 °C, protein lysates were collected and stored at -80°C.

For co-immunoprecipitation experiments, cellular pellet was suspended in a different lysis buffer (25 mM Tris-HCl pH 8, 125 mM NaCl, 10% Glycerol, 0.5% NP-40) complemented with Protease Inhibitor Cocktail 1x (P8340, Sigma-Aldrich), 10 mM sodium butyrate (B5887, Sigma-Aldrich), 5 mM sodium fluoride (7681-49-4, Sigma-Aldrich), 1 mM sodium orthovanadate (S6508, Sigma-

Aldrich), 1x phenylmethylsulfonyl fluoride (PMSF-RO Roche). Samples were incubated at 4 °C for 15 minutes, sonicated (30% amplitude, 10 seconds ON, 30 seconds OFF at 4 °C) and centrifuged at 8385 xg, 4 °C for 10 minutes; supernatants were collected and stored at -80 °C. Lysate quantification was performed through the Bradford reagent (B6916, Sigma-Aldrich) or the Pierce BCA Protein Assay Kit (23227 Thermo Fisher Scientific), according to manufacturer's instructions. Sample absorbance was measured at 570 nm for Bradford and at 460 nm for the Pierce BCA Protein Assay Kit, using the Microplate Reader EL311 (214891, BioTek Instruments, Inc).

## 5. Immunoblotting

Equal amounts of proteins (10-30 µg, as specified in the immunoblotting results figure legends) were separated on NuPAGE™ 10% Bis-Tris Protein Gels, (NP0301BOX, Life Technologies), Bolt™ 4 to 12%, Bis-Tris, 1.0 mm Mini Protein Gel (NW04122BOX, Thermo Fischer Scientific) or 7% tris-tricine gels using 200 V for 30 minutes. Proteins were transblotted to nitrocellulose membranes using 120 V for 10 minutes (PB7320, Thermo Fischer Scientific) through the Electrophoresis Power Supply (EPS301, Thermo Fischer Scientific). After incubation with 5% nonfat milk in Tris Buffered Saline (50 mM Tris-Cl, 150 mM NaCl, pH 7,5) with 0.1% Tween-20 (T-TBS) for 1 hour to block aspecific sites, membranes were incubated with rabbit primary antibodies against human antigens: LC3 (dilution 1:1000; ab48394, Abcam), PACSIN2 (1:100 dilution; TA325022, OriGene), GAPDH (1:500 dilution, sc20357, Santa Cruz), actin (1:3000 dilution; ab218787, Abcam), SQSTM1/P62 (1:250 dilution; GT381, GeneTex), PARP1 (1:1000 dilution; #9532, Cell Signaling Technology) or mouse primary antibody against human TPMT (1:500 dilution; sc-374154, Santa Cruz). After washing 3 times for 10 minutes with Tween Tris buffered saline (28360, Thermo Fischer Scientific), membranes were incubated with appropriate horseradish peroxidase (HRP)-conjugated secondary anti rabbit IgG (1:10000 dilution; AP132P, Merck) or HRP-conjugated secondary anti mouse IgG (1:20000 dilution; anti-mouse IgG, HRP-linked Antibody #7076, Cell signaling). Immunocomplexes were visualized by chemiluminescence, using the LiteAblo TURBO Extra Sensitive Chemiluminescent Substrate (EMP012001, Euroclone) and using photographic films (Carestream Kodak Biomax, Z373508, Merck) or the ChemiDoc gel imaging system (Bio-Rad). Protein levels were quantified by densitometry normalized against actin. Signal intensities were quantified using ImageJ and normalized for the signal intensity of the loading control in the same lane.

## 6. RNA extraction

Total RNA was extracted from patients' biopsies using 1 ml of TRIZOL reagent. Two hundred µL of chloroform (288306, Sigma-Aldrich) were added and, after 3 minutes of incubation at room temperature, a centrifugation at 12000 xg for 15 minutes at 4 °C was performed. The supernatant was used for RNA purification through the PureLink® RNA Mini Kit (12183018A, ThemoFisher). Briefly, ethanol 70% was added to the aqueous phase of RNA and the sample was mixed and added to the column of the kit and centrifuged at 12000 xg for 1 minute at room temperature. During this process the RNA was retained by the filter of the column; then, two washes were performed with the wash buffer of the kit and samples were centrifuged twice at 12000 ×g for 1 minute at room temperature. Finally, RNA was eluted using sterile RNase-free water present in the kit by centrifugation for 2 min at 12000 xg and at room temperature. RNA concentration and purity were evaluated using the NanoDrop 2000 spectrophotometer (Thermo Fisher Scientific).

## 7. Gene expression analysis

The RNA reverse transcription reaction into cDNA was performed using the High Capacity RNA-to-cDNA Kit (4387406, Thermo Fisher Scientific). Up to 1 µg RNA was retro-transcripted in a total reaction volume of 20 µL, containing 10 µL of 2X Reaction Mix, 1 µL of 20X RT Enzyme and RNase/DNase-free water up to reach the final volume.

Gene expression analysis was performed by quantitative real-time PCR using TaqMan Gene Expression Assay probes for *PACSIN2* (Hs00200589_m1, ThermoFisher) and the *ribosomal protein lateral stalk subunit P0* (*RPLP0*, Hs99999902_m1, ThermoFisher), as reference gene. Results were expressed as base 10 logarithm of the ΔCt of the relative expression (RE).

## 8. LC3 interacting region (LIR) identification

The examination of the primary structure for PACSIN2 protein to identify a possible LIR domain in the sequence was performed through an *in silico* analysis performed using the iLIR database. (Mizushima et al., 2010) (Jacomin et al., 2016) As positive control, we performed the same analysis on SQSTM1/P62 primary sequence to identify the LIR domain present in this protein (Pankiv et al.,

2007); finally, this *in silico* analysis was performed on the ABL1 primary sequence, used as negative control.

## 9. Plasmids expansion and purification

OmicsLink™ Expression-Ready ORF cDNA Vector presenting the eGFP reporter gene (Cat# EX-EGFP-M39), and vector carrying the *PACSIN2* wild type and mutated cDNA (Cat# CS-I2075-M39 and CS-I2075-M39-01, respectively) were purchased from Gene Copoeia. The *PACSIN2* wild type cDNA sequence (NCBI Reference Sequence NM_007229.3) encoded for the protein sequence shown. (Figure 8A). For mutated *PACSIN2*, the nucleotide sequence TTCGAGAAGATC in position 325 was mutated into **GCA**GAGAAG**GCA,** resulting in a PACSIN2 protein with both the phenylalanine in position 109 and the isoleucine in position 112 replaced by alanine. (Figure 8B)

a)

**> Wild type PACSIN2**

MSVTYDDSVGVEVSSDSFWEVGNYKRTVKRIDDGHRLCSDLMNCLHERARIEKAYAQQLTEWARRWRQLVEKGPQYGTVEKAWMAFM
SEAERVSELHLEVKASLMN**DDFEKI**KNWQKEAFHKQMMGGFKETKEAEDGFRKAQKPWAKKLKEVEAAKKAHHAACKEEKLAISREA
NSKADPSLNPEQLKKLQDKIEKCKQDVLKTKEKYEKSLKELDQGTPQYMENMEQVFEQCQQFEEKRLRFFREVLLEVQKHLDLSNVA
GYKAIYHDLEQSIRAADAVEDLRWFRANHGPGMAMNWPQFEEWSADLNRTLSRREKKKATDGVTLTGINQTGDQSLPSKPSSTLNVP
SNPAQSAQSQSSYNPFEDEDDTGSTVSEKDDTKAKNVSSYEKTQSYPTDWSDDESNNPFSSTDANGDSNPFDDDATSGTEVRVRALYD
YEGQEHDELSFKAGDELTKMEDEDEQGWCKGRLDNGQVGLYPANYVEAIQ

b)

**> Mutated PACSIN2**

MSVTYDDSVGVEVSSDSFWEVGNYKRTVKRIDDGHRLCSDLMNCLHERARIEKAYAQQLTEWARRWRQLVEKGPQYGTVEKAWMAFMS
EAERVSELHLEVKASLMN**DDAEKA**KNWQKEAFHKQMMGGFKETKEAEDGFRKAQKPWAKKLKEVEAAKKAHHAACKEEKLAISREANS
KADPSLNPEQLKKLQDKIEKCKQDVLKTKEKYEKSLKELDQGTPQYMENMEQVFEQCQQFEEKRLRFFREVLLEVQKHLDLSNVAGYK
AIYHDLEQSIRAADAVEDLRWFRANHGPGMAMNWPQFEEWSADLNRTLSRREKKKATDGVTLTGINQTGDQSLPSKPSSTLNVPSNPA
QSAQSQSSYNPFEDEDDTGSTVSEKDDTKAKNVSSYEKTQSYPTDWSDDESNNPFSSTDANGDSNPFDDDATSGTEVRVRALYDYEGQ
EHDELSFKAGDELTKMEDEDEQGWCKGRLDNGQVGLYPANYVEAIQ

***Figure 8: PACSIN2 amino acid sequences.*** *A) PACSIN2 wild type protein B) Mutated PACSIN2 protein sequence. LIR motif is highlighted in bold; in red the amino acids of the LIR domain that have been substituted with alanine to disrupt the function of the LIR motif are highlighted.*

Plasmids were expanded using DH5α *E. coli* competent cells grown in different media: the Luria-Bertani broth (NaCl 10 g/L, Tryptone, 10 g/L,Yeast Extract, 5 g/L) for bacteria transfected with the EX-EGFP-M39 vector and the Terrific Broth (Tryptone, 12 g/L, 24 g/L, Yeast Extract, Glycerol 0.4%, $K_2HPO_4$ 72mM, $KH_2PO_4$ 17 mM) for the *E.coli* transfected with the CS-I2075-M39 and CS-I2075-M39-01, respectively. The media used for transfected *E. coli* expansion were completed with ampicillin (69-53-4, Sigma-Aldrich) 10 µg/µL to select bacteria presenting the transfected plasmids. Then, plasmids were purified using the EndoFree® Plasmid Maxi Kit (12362, Qiagen) and eluted in endotoxin-free TE Buffer of the kit. Plasmid quantification was performed using the NanoDrop 2000 spectrophotometer (Thermo Fisher Scientific).

## 10. Transient cell transfection

LS180 MOCK were seeded in RPMI-1640 (ECB9006L, Euroclone) without antibiotics at a concentration of $1x10^6$ cells/well; cells at 80-90% confluence were transfected with 7 µg of OmicsLink™ Vectors using 6 µl of Lipofectamine 2000 Transfection Reagent (11668019, Thermo Fisher Scientific) and 2 ml of Optimem medium (31985070, Thermo Fisher Scientific) and incubated for 48 hours. Then, cells were washed twice with PBS and centrifuge at 600 xg for 5 minutes. Pellets were collected and lysed, as described above.

## 11. Co-immunoprecipitations

Co-immunoprecipitations were performed using LS180 MOCK cells and LS180 cells transfected to overexpress the wild type or the mutated PACSIN2. Protein G Sepharose 4 Fast Flow (17-0618-01, Merck) was incubated 1 hour with 4 µg of antibody (anti-human LC3 IgG (ab48394, Abcam), anti-human PACSIN2 IgG (TA325022, OriGene) or rabbit IgG, polyclonal isotype control (ab37415, Abcam)), blocked 1 hour with bovine serum albumin 1 mg/ml and then incubated for 3 hours with 500 µg of cell lysates. After washing with lysis buffer, beads were eluted with sample buffer (B0007, Thermo Fisher Scientific) completed with 1 M 1,4-dithiothreitol (DTT), boiled for 5 minutes at 95 °C and loaded on gels. For the immunoblotting of LC3-II, the NuPAGE™ 10% Bis-Tris Protein precast gels (NP0301BOX, Life Technologies) home-made 7% tris-tricine gels were used to improve separation between PACSIN2 (expected molecular weight: 56 kDa) and the heavy chains of the primary antibodies (expected molecular weight: 55 kDa).

## 12. Drug sensitivity assay

NALM6 or LS180 cell lines were seeded in 96-well plates at 20000 cells/well and 5000 cells/well, respectively (in a final volume of 100 µl). Subsequently, 100 µl per well of drugs (mercaptopurine, tunicamycin, thioguanine, fluorouracil) at known concentrations (range in Table 1) or cell medium in controls were added. Plates were incubated for 72 hours at 5% $CO_2$ and 37 °C. During the last 4 hours of incubation, 20 µl of 3-4,5-dimethylthiazol-2,5-diphenyl tetrazolium bromide (MTT, M2128, Sigma-Aldrich) was added in each well (0.5 mg/ml). After incubation, supernatants were removed and salt precipitates were suspended in 100 µl of dimethyl sulfoxide (472301, Sigma-Aldrich); absorbance was measured with a Microplate Reader EL311 (214891, BioTek Instruments, Inc) at 570-630 nm wavelength. Results were expressed as percentages of survival according to the absorbance ratio between treated and untreated condition (after blank subtraction), and EC50 values were calculated on dose-response curves.

## 13. Mitochondrial membrane potential measurement

LS180 cells were seeded in 96-well plates at 5000 cells/well at a final volume of 100 µl. After 24 hours, 100 µl of mercaptopurine (final concentrations in culture well: 1.25 µM and 2.5 µM) were added and incubated for 24 or 48 hours; cell incubation with 100 µl of doxorubicin at the final concentration of 5 µM for 24 hours was used as positive control. Thirty minutes before the incubation end, wells were washed twice with 100 µl PBS and 50 nM of DiOC6 probe (3,3′-dihexyloxacarbocyanine iodide, 318426, Sigma-Aldrich) were added and incubated 30 minutes at 37 °C. Finally, absorbance was measured at 485/520 nm using the Microplate Reader EL311 (214891, BioTek Instruments, Inc).

## 14. HPLC-UV analysis

LS180 cells were seeded at 1.7 x $10^6$ in 7 ml of RPMI medium and after 24 hours were treated with mercaptopurine 2.5 µM for 24 or 48 hours. Cells were washed with PBS, centrifuged 5 minutes at 600 xg; pellets were collected, suspended in 500 µl of milliQ water, freezed and thawed to lyse samples. Thiopurine metabolites were quantified using a previously described method. (Dervieux & Boulieu, 1998) In particular, before the HPLC-UV analysis, samples were prepared adding 10 µl of

500 mg/ml DTT (10197777001, Sigma-Aldrich). Then, 70% perchloric acid was added; samples were mixed and centrifuged at 22 °C for 15 minutes at 16100 xg and then incubated 1 hour at 95 °C to allow the acid hydrolysis of samples. Samples were stored for 20 minutes at -20 °C; then they were injected to the HPLC-UV system (Agilent 1260 Infinity II, Agilent) presenting the Zorbax Eclipse Plus C18 (5 μm, 250 mm x 4,6 mm) chromatographic column (Agilent). For the chromatographic analysis, a buffer composed by $K_3PO_4$ (0.02 M, pH = 3.5) and methanol was used as mobile phase to perform a chromatographic run lasting 18 minutes with 1.1 mL/minute flow. The thiopurine metabolites TGN and MMPN were detected evaluating samples absorbance at 340 nm and 304 nm, as peaks occurring at 8.5 and 13.5 minutes, respectively.

## 15. Statistical analysis

Statistical analysis was performed with the software PRISM version 7.0. For immunoblotting and gene expression assay differences were evaluated using t-test, whereas for cytotoxicity assay and mitochondrial membrane potential measurement assay the two-way ANOVA was used. For all continuous variables, results are reported as mean and standard error. All experiments were performed with at least three biological replicates.

# RESULTS

## 1. Cell line characterization

Before starting experiments, cell lines were characterized by western blot to verify the presence of the expected genetic modifications. In particular, PACSIN2 KD was evaluated in both NALM6 and LS180 cells using an anti-human PACSIN2 antibody, whereas the overexpression of TPMT was verified only in NALM6 cell lines using an anti-human TPMT antibody. The immunoblotting results showed that *PACSIN2* was completely silenced in NALM6 cells, whereas the PACSIN2 band was strongly reduced in LS180 cells, confirming the optimal silencing of *PACSIN2* gene in these *in vitro* models. The western blot results for TPMT revealed the presence of a 36 kDa band in all NALM6 cell lines; this signal corresponds to the endogenous isoform of TPMT. The presence of TPMT overexpression was successfully identified both in NALM6 *1 and NALM6 KD*1 through the detection of a western blot band at 38kDa, corresponding to the exogenous isoform of the protein. The difference in the molecular weight detected between the endogenous and exogenous isoform of TPMT is due to the presence of a flag tag (D-D-K) in the overexpressed isoform of TPMT. As expected, in LS180 cell lines only the endogenous isoform of TPMT was detected. (Figure 9)

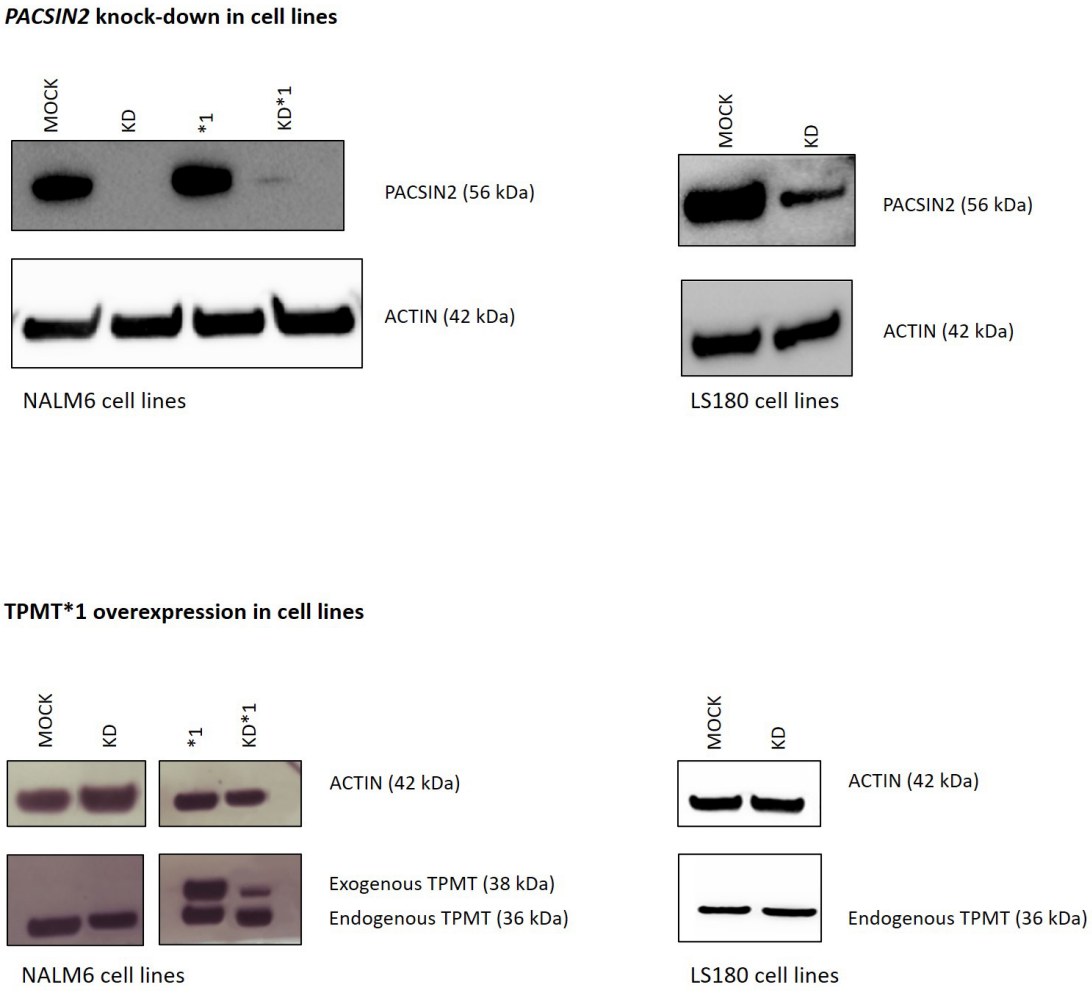


***Figure 9: cell line characterization:*** *the evaluation of PACSIN2 and TPMT protein expression in LS180 and NALM6 cell lines confirmed the expected genetics modifications in these in vitro models.*

## 2. Autophagy is increased after *PACSIN2* KD

To determine whether PACSIN2 plays a role in autophagy, western blot assays were performed to evaluate the amount of the autophagic markers LC3-II and SQSTM1/P62 in both NALM6 and LS180 cell lines (MOCK and KD).

The immunoblotting results showed that LC3-II was significantly increased in *PACSIN2* KD cells compared to MOCK controls in both NALM6 (fold change 2.10 ± 0.18, P = 0.0031, figure 10a) and LS180 (fold change 1.3 ± 0.09, P = 0.028, figure 10b). In NALM6 KD cells, LC3-I was also significantly increased compared to NALM6 MOCK cells (fold change 1.70 ± 0.13, P = 0.0045, figure 10a). Moreover, both NALM6 KD and LS180 KD cells presented lower SQSTM1/P62 levels compared to MOCK cells (NALM6: fold change 0.67 ± 0.09, P= 0.023, figure 10c; LS180: fold change 0.47 ± 0.14, P = 0.019, figure 10d). Taken together, the immunoblotting results for LC3-II

and SQSTM1/P62 are coherent in showing that the lack of PACSIN2 increases the autophagic process and suggest that PACSIN2 protein is able to negatively modulate autophagy.

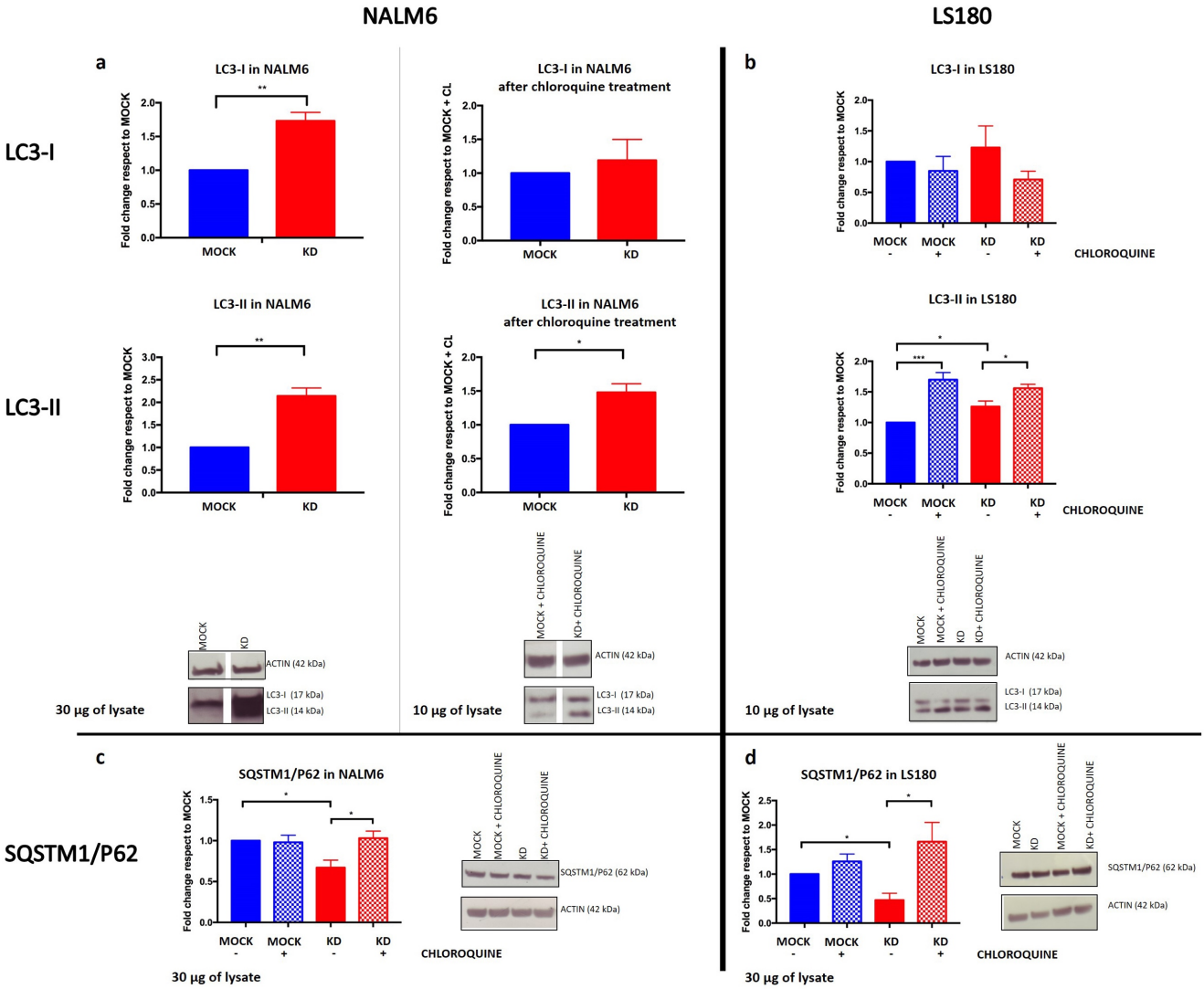


***Figure 10: autophagy is increased after PACSIN2 KD in both NALM6 and LS180 cell lines.*** *A) In NALM6 KD cells there was an increase of both LC3-I and LC3-II compared to MOCK control cells. After chloroquine treatment, a higher amount of LC3-II was found in both NALM6 MOCK and KD cell lines and this increase was higher in NALM6 KD cells. For these western blots, 30 µg of cell lysates were used under basal condition, whereas to detect LC3 after chloroquine treatment the loaded amount of lysates was reduced to 10 µg to avoid signal saturation. B) LC3-II levels were higher in LS180 KD cells compared to MOCK, under basal condition. After 30 µM of chloroquine exposure, both LS180 MOCK and LS180 KD cells showed higher LC3-II levels and these amounts were significantly higher in LS180 KD cells. For these immunoblotting assays, we used 10 µg of cell lysates to evaluate LC3-II amount. C) NALM6 KD cells showed lower SQSTM1/P62 levels compared to control cells under basal condition; 24 hours of chloroquine treatment rescued SQSTM1/P62 levels in NALM6 KD cells. In these experiments, 30 µg of cell lysates were loaded to detect SQSTM1/P62 levels. D) LS180 KD cells presented lower SQSTM1/P62 levels compared to control cells under basal condition; moreover, 24 hours of chloroquine treatment increased SQSTM1/P62 amount, particularly in LS180 KD cells. For these western blots 30 µg of cell lysates were loaded to detect SQSTM1/P62. All experiments were performed at least three times. * p-value ≤ 0.05, ** p-value ≤ 0.01, *** p-value ≤ 0.001.*

## 3. *PACSIN2* could play a role in first phases of autophagy

In order to understand the potential molecular mechanism at the basis of PACSIN2 regulation of the autophagic flux, the amount of LC3-II and SQSTM1/P62 proteins was evaluated in NALM6 and LS180 cell lines in the presence of 30 μM chloroquine, an autophagy inhibitor that impairs the last phases of autophagy, impairing autophagosomes fusion with lysosomes. Since chloroquine interferes with the later phases of the autophagic flux, it is expected that LC3-II and SQSTM1/P62 accumulate after drug exposure. Four hours of chloroquine exposure increased LC3-II levels both in MOCK and KD cells; the increase in LC3-II amount was significantly higher in *PACSIN2* KD compared to MOCK, both in NALM6 (fold change 1.5 ± 0.13, P = 0.020, figure 10a) and LS180 cells (fold change 0.93 ± 0.03, P = 0.035, figure 10b), suggesting that PACSIN2 could inhibit autophagy acting at the beginning of the autophagic flux. However, 4 hours of chloroquine treatment did not affect SQSTM1/P62 levels, suggesting the need of a longer chloroquine exposure to affect SQSTM1/P62 levels. Indeed, after 24 hours of 30 μM chloroquine exposure, SQSTM1/P62 was increased both in NALM6 KD and LS180 KD cells compared to MOCK cell (NALM6: fold change 1.57 ± 0.1, P= 0.047, figure 10c; LS180: fold change 3.94 ± 1.8, P = 0.046, figure 10d), indicating again that PACSIN2 could be involved in the first stages of autophagy.

## 4. Colon samples of IBD pediatric patients showed an inverse correlation among PACSIN2 amount and both inflammation and autophagy levels

Since impaired autophagy is associated with pathological conditions such as IBD, (S. Kim et al., 2019) the amount of LC3-II and both PACSIN2 mRNA and protein levels was evaluated in inflamed and non-inflamed colon biopsies of IBD pediatric patients at diagnosis, before the beginning of thiopurine therapy. The cohort consists of 20 pediatric patients (mean age: 13.5 ± 0.75 years), equally distributed by gender (10 females (50%)), 11(55%) presenting Crohn's disease and 9 (45%) ulcerative colitis. In particular, for 15 of these patients, biopsies were used for gene expression analysis and for 6, biopsies were available to evaluate protein expression levels by western blot. Therefore, for only one patient, biopsies were available for both analyses.

Compared to non-inflamed samples, inflamed colon tissues showed a decreased amount of both PACSIN2 mRNA (fold change of 2.2 ± 0.34; P = 0.0084, figure 11a) and protein (fold change 0.65 ± 0.09, P = 0.02, Fig 11b) and higher amount of LC3-II protein (fold change 1.9 ± 0.05, P = 0.0034,

figure 11b). Taken together, these results indicated an inverse correlation between PACSIN2 amount and autophagy levels, supporting previous results on *in vitro* models, associating reduced PACSIN2 to increased autophagy.

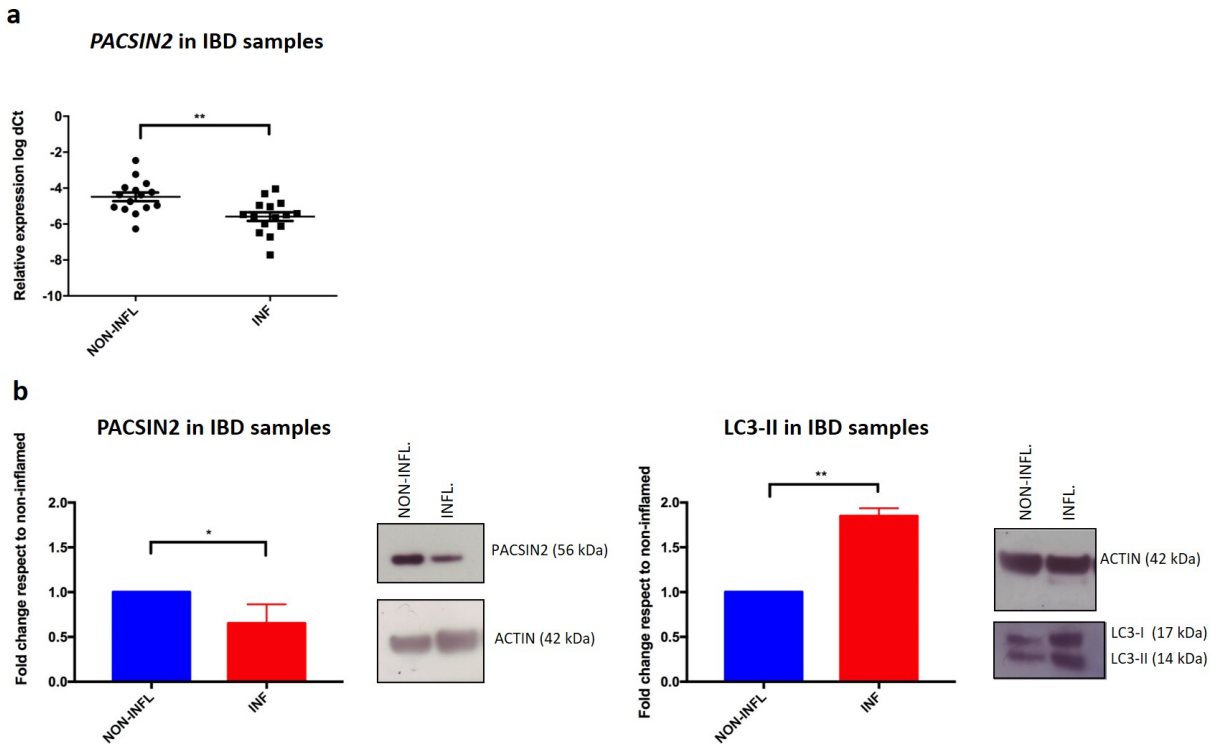


***Figure 11: PACSIN2 decreases in presence of high autophagy and inflammation levels in colon biopsies of inflammatory bowel disease (IBD) patients****. A) Comparison of PACSIN2 mRNA levels between colon samples of inflamed and non-inflamed biopsies on a cohort of 15 IBD pediatric patients: PACSIN2 was decreased in inflamed colon tracts compared to non-inflamed ones. B) PACSIN2 protein expression level decreased and LC3-II amount increased in 6 inflamed biopsies. * p-value ≤ 0.05, ** p-value ≤ 0.01.*

## 5. *In silico* identification of the LIR domain present in PACSIN2

The *in silico* analysis performed using the iLIR database revealed the presence of one LIR motif (D-D-F-E-K-I) on the amino acidic sequence of PACSIN2 protein, suggesting a potential physical interaction between PACSIN2 and LC3. As control, the analysis with the iLIR database was performed also on the SQSTM1/P62 and ABL1 protein sequences. As expected, for SQSTM1/P62 a LIR domain (D-D-W-T-H-L) was identified, whereas no LIR motifs were found for the ABL1 protein sequence.

## 6. PACSIN2-LC3 protein-protein interaction: experimental validation

In order to evaluate whether PACSIN2 interacts physically with LC3-II, co-immunoprecipitations of the two proteins were performed in LS180 MOCK cells, under basal levels of endogenous PACSIN2 (Figure 12A) and after overexpression of wild type and mutated PACSIN2 protein (Figure 12B).
The immunoblotting results obtained under basal condition showed the presence of a large amount of co-immunoprecipitated LC3-II after the immunoprecipitation of PACSIN2 protein, confirming the predicted physical interaction between these two proteins.
The possible role of the LIR motif of PACSIN2 in the physical biding between PACSIN2 and LC3-II was further evaluated through co-immunoprecipitations in LS180 MOCK cells transiently transfected with a plasmid coding for PACSIN2 wild type isoform or one presenting PACSIN2 with a mutated LIR domain. In particular, the mutation was obtained through the substitution of the third and the last amino acid of the LIR motif with alanine in order to disrupt the function of this domain (Figure 8). As control, cells transfected with an empty plasmid vector were used. The cells transfected with the plasmid coding for wild type PACSIN2 or the plasmid presenting the mutated isoform of PACSIN2 showed a larger PACSIN2 amount compared to cells transfected with the empty vector, indicating a successful transfection and PACSIN2 overexpression. The amount of co-immunoprecipitated LC3-II was clearly reduced in cells presenting the mutated isoform of PACSIN2 compared to those with the wild type isoform of PACSIN2 (figure 12b), suggesting a key role of the LIR motif in the physical interaction between PACSIN2 and LC3-II.
Taken together, these results confirmed the *in silico* previsions, showing a protein-protein interaction between PACSIN2 and LC3-II mediated by the LIR domain. These results are consistent with the hypothesis that PACSIN2 could play its role at the beginning of the autophagic flux, when LC3 is the key autophagic marker involved.

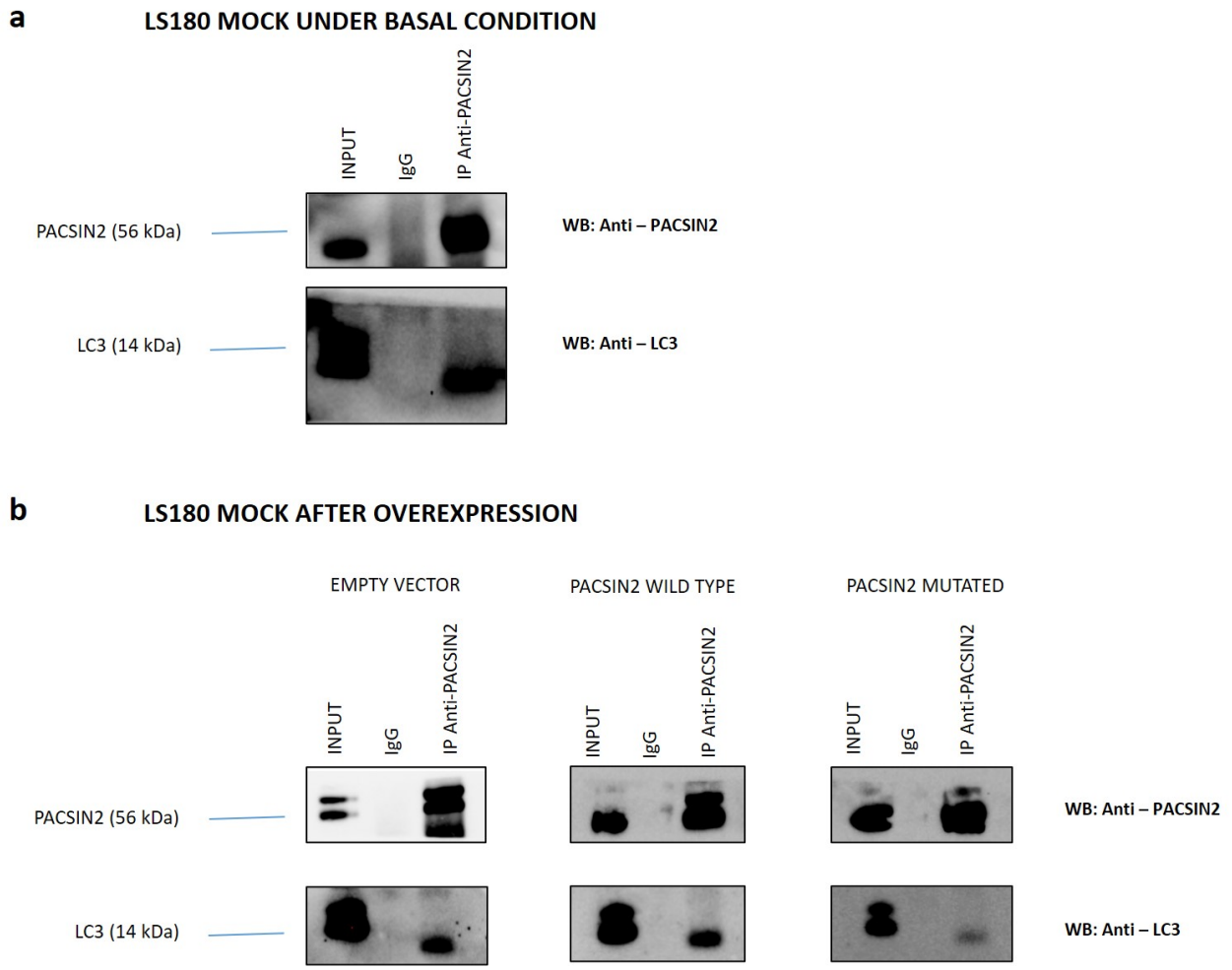


***Figure 12: the protein-protein interaction between PACSIN2 and LC3-II is mediated by the LIR motif of PACSIN2.*** *A) After PACSIN2 immunoprecipitation, LC3-II protein was detected. B) LC3-II level was reduced in presence of immunoprecipitated PACSIN2 with mutations in the LIR motif.*

## 7. *PACSIN2* KD affects the unfolded protein stress response, evaluated as tunicamycin sensitivity

Autophagy could be used by cells as a survival mechanism in response to different stress sources, such as ER stress; however elevated stress levels lead to cell death. The cytotoxic effects of the ER-stress inducer tunicamycin, whose exposure results in autophagy stimulation, was evaluated both in NALM6 and LS180 cells. Interestingly, NALM6 KD cells presented an increased sensitivity to tunicamycin (-Log IC50 NALM6 MOCK vs -Log IC50 NALM6 KD: 6.794 M ± 0.05 vs 7.064 M ± 0.06, P = 0.0279, Fig. 13a); also TPMT overexpression increased tunicamycin sensitivity in these cells, whereas the presence of both modifications (*PACSIN2* KD *1 cell line) did not further increase tunicamycin cytotoxicity (figure 13a). In contrast, the presence of *PACSIN2* KD did not affect tunicamycin sensitivity in LS180 cells (figure 13b).

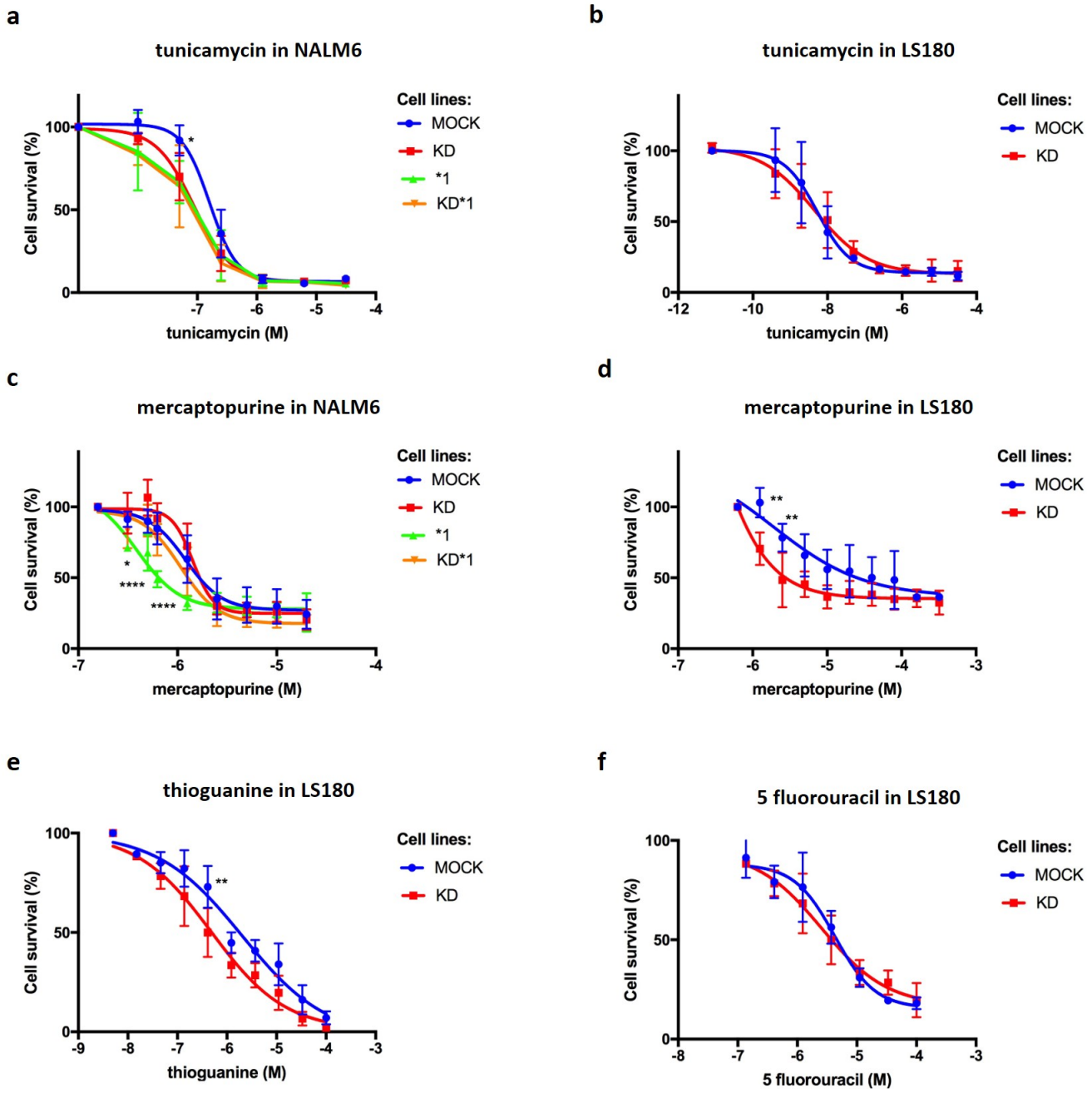


***Figure 13: cytotoxicity assay results on NALM6 and LS180 cells.*** *A) Tunicamycin sensitivity results on NALM6 showed that NALM6 KD cells were more sensitive to this drug than control cells. No statistically significant difference in drug sensitivity was found in presence of TPMT overexpression. B) Cytotoxicity results for tunicamycin on LS180 cells showed no statistically significant difference in presence of PACSIN2 KD. C) NALM6 sensitivity to mercaptopurine: NALM6*1 was the most sensitive cell line to mercaptopurine after 72 hours of drug exposure and differed significantly from control cells; interestingly, NALM6 KD*1 cells showed similar sensitivity to control cells, suggesting a role of PACSIN2 on TPMT activity in presence of its overexpression. D) LS180 cytotoxicity results for mercaptopurine: LS180 KD cells were more sensible than control cells. E) Sensitivity results for thioguanine showed an increased cytotoxicity in LS180 KD cells compared to LS180 MOCK cells. F) Cytotoxicity results for 5-fluorouracil on LS180 cells showed no statistically significant difference in presence of PACSIN2 KD. All experiments were performed at least three times. * p-value ≤ 0.05, ** p-value ≤ 0.01, *** p-value ≤ 0.001, **** p-value ≤ 0.0001.*

## 8. *PACSIN2* KD impact on thiopurine sensitivity

In order to evaluate the possible role of *PACSIN2* on mercaptopurine sensitivity, also in presence of TPMT overexpression, cell viability was evaluated after 72 hours of drug exposure. The MTT assay results showed that NALM6*1 was the most sensitive cell line to mercaptopurine cytotoxic effects and differed significantly from NALM6 MOCK (-LogIC50 *1 vs MOCK: 6.4 M ± 0.08 vs 5.9 M ± 0.04, $P < 0.0001$); no difference in mercaptopurine sensitivity was detected between NALM6 MOCK and NALM6 KD. Interestingly, NALM6 KD*1 showed a comparable cytotoxic dose-response profile to NALM6 MOCK, indicating a possible role of PACSIN2 on TPMT activity in presence of its overexpression. (Figure 13c) Cytotoxicity results showed that LS180 KD cells were more sensitive to mercaptopurine than LS180 MOCK (-Log IC50 LS180 KD: 5.8 M ± 0.04 vs LS180 MOCK: 5.3 M ± 0.1, $P < 0.0001$ figure 13d), suggesting the hypothesis of an intestinal cell specific role of PACSIN2 in thiopurine-mediated *in vitro* cytotoxicity. Interestingly, LS180 KD cells showed an increased sensitivity to thioguanine compared to the LS180 MOCK (-Log IC50 LS180 MOCK: 5.69 M ± 0.22; LS180 KD: 6.32 M ± 0.11, $P < 0.0014$, Figure 13e), suggesting an effect of PACSIN2 on thiopurine cytotoxicity in the intestinal cells. On the basis of these results, the LS180 cells sensitivity to another antimetabolite drug was evaluated to investigate the possible role of PACSIN2 in the cytotoxicty of non-thiopurine antimetabolites. The MTT assay results showed no significant differences in drug sensitivity between LS180 MOCK and LS180 KD cells (Figure 13f), supporting the hypothesis a specific role of PACSIN2 in the cytotoxic mechanisms of thiopurines.

## 9. *PACSIN2* KD counteracts mercaptopurine-induced autophagy inhibition

Because the intestinal LS180 KD cells showed higher autophagy and higher mercaptopurine cytotoxicity than LS180 MOCK, the potential impact of mercaptopurine exposure on autophagy was investigated. In particular, cells were exposed to mercaptopurine at the concentrations displaying a statistically different cytotoxicity in the MTT assay (i.e. 1.25 μM and 2.5 μM), and LC3-II levels were evaluated after 24 or 48 hours of drug exposure.

The immunoblotting results performed after 24 hours of mercaptopurine exposure showed a reduction in the LC3-II amount, both in LS180 MOCK (fold change 1.25 μM: 0.72 ± 0.05, P = 0.0057; 2.5 μM: 0.59 ± 0.08, P = 0.0071, figure 14a) and LS180 KD cells (fold change 1.25 μM: 0.85 ± 0.02, P = 0.0037; 2.5 μM: 0.84 ± 0.02, P = 0.048, figure 14a) compared to untreated samples. Also 48 hours of mercaptopurine treatment decreased LC3-II in both LS180 MOCK (fold change 1.25 μM MP: 0.53 ± 0.04, P = 0.0003; 2.5 μM MP: 0.14 ± 0.05, P < 0.0001, figure 14b) and LS180 KD cells (fold change 1.25 μM MP: 0.71 ± 0.12, P = 0.023; 2.5 μM MP: 0.60 ± 0.04, P = 0.004, figure 14b), suggesting that mercaptopurine is able to reduce autophagy in these cellular models. Furthermore, LS180 KD cells showed higher LC3-II levels compared to MOCK cells after both 24 hours (fold change untreated: 2.12 ± 0.06, P < 0.0001; 1.25 μM: 2.52 ± 0.3, P = 0.0004; 2.5 μM: 3.1 ± 0.2, P = 0.0007, figure 14a) and 48 hours (fold change untreated: 1.24 ± 0.07, P = 0.03, 1.25 μM: 1.62 ± 0.3, P = 0.035; 2.5 μM: 6.7 ± 2.35, P = 0.0015, Fig. 14b), consistently to what was observed in confluent untreated cells (figure 10b).

Taken together, these western blot results suggested that mercaptopurine exposure is able to reduce autophagy in LS180 cells; interestingly, this effect is less evident in LS180 KD cells, in line with previous evidences of PACSIN2 as a negative regulator of autophagy.

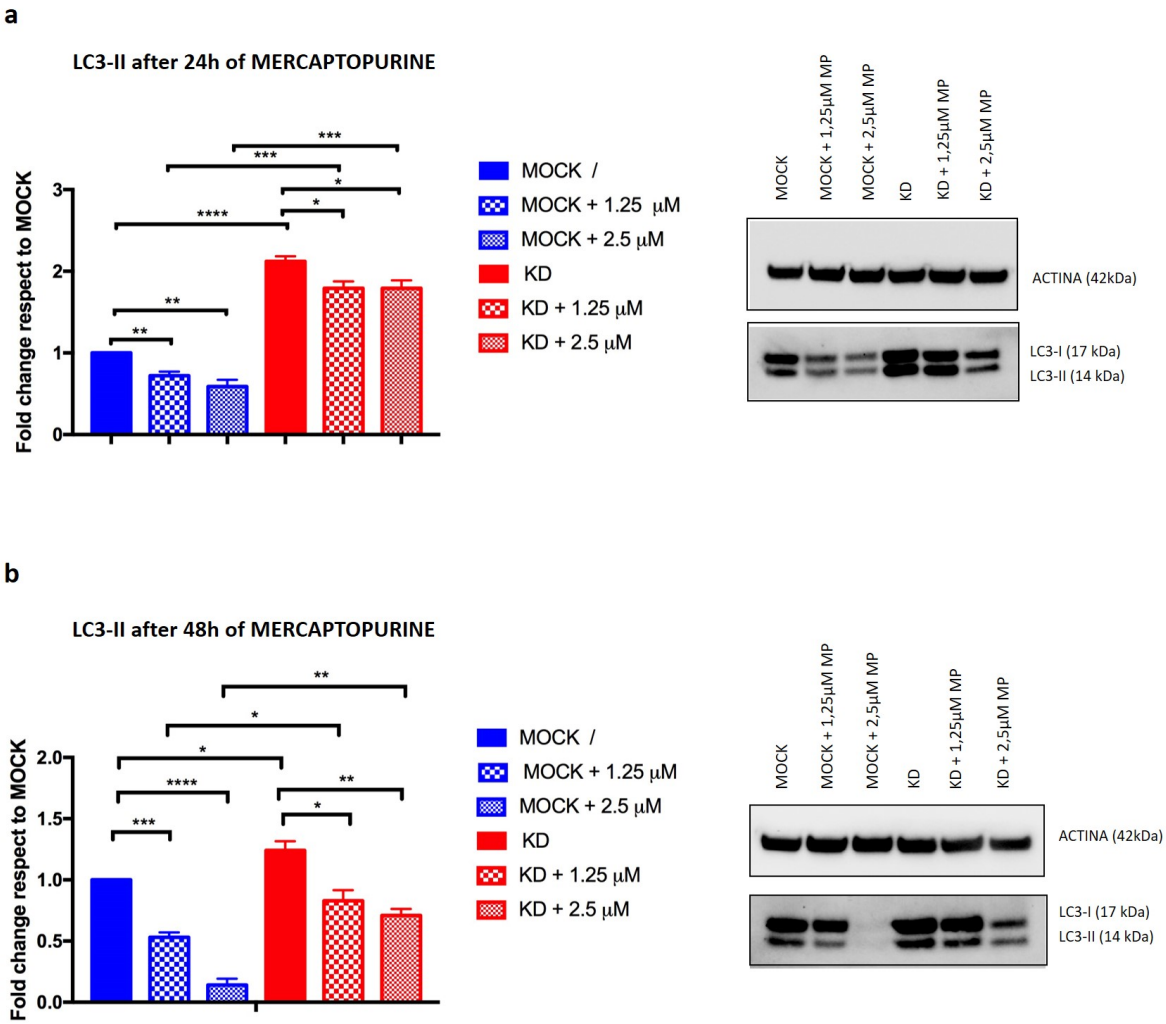


***Figure 14: the effect of both PACSIN2 KD and mercaptopurine treatment on autophagy.*** *A) Immunoblotting results of the autophagic marker LC3-II after 24 hours of 1.25 µM and 2.5 µM mercaptopurine treatment in LS180 cell lines. LS180 KD cells presented higher LC3-II levels compared to MOCK cells after 24 hours. Mercaptopurine treatment for 24 hours decreased the amount of LC3-II in LS180 MOCK cells compared to untreated cells and LS180 KD. B) LC3-II amount was reduced after 48 hours of 1.25 µM, 2.5 µM in LS180 cell lines. LS180 KD cells showed higher levels of LC3-II compared to MOCK cells after 48 hours. Mercaptopurine exposure decreased LC3-II levels in both LS180 MOCK and LS180 KD cells, even if the decrease was less evident in LS180 KD cells. Western blot experiments were performed using 10 µg of cell lysate. All experiments were performed at least three times. All experiments were performed at least three times. * p-value ≤ 0.05, ** p-value ≤ 0.01, *** p-value ≤ 0.001, **** p-value ≤ 0.0001.*

## 10. Both mercaptopurine treatment and *PACSIN2* KD increased apoptosis in intestinal cells

The potential impact of *PACSIN2* KD on apoptosis was investigated after cell exposure to mercaptopurine at 1.25 µM and 2.5 µM, evaluating the level of cleaved PARP1 in intestinal LS180 cells by western blot. LS180 KD cells showed higher apoptosis compared to control MOCK cells under basal condition after 24 hours of cell growth (fold change 2.00 ± 0.26, P = 0.020, figure 15a); interestingly, no statistically significant difference in cleaved PARP1 amount between LS180 MOCK

and L180 KD cells was detected after 48 hours of cell growth under basal condition, indicating the presence of a similar apoptotic level in both cell lines at this time point.

Treatment with 1.25 μM mercaptopurine for 24 hours decreased apoptosis in both LS180 MOCK (fold change 0.32 ± 0.02, P<0.0001) and LS180 KD cells (fold change 1.25 μM: 0.95 ± 0.07, P = 0.019), compared to untreated controls, whereas exposure to 2.5 μM mercaptopurine led to higher apoptosis both in LS180 MOCK (fold change 2.5 μM: 5.21 ± 0.54, P = 0.0014, figure 15a) and LS180 KD cells (fold change 2.5 μM: 12.3 ± 0.51, P<0.0001, figure 15a). Interestingly, a consistently higher apoptosis was detected in LS180 KD cells exposed to mercaptopurine, compared to MOCK (fold change 1.25 μM: 2.97 ± 0.31, P = 0.001; 2.5 μM: 2.41 ± 0.2, P = 0.0007, figure 15a) after 24 hours of drug exposure. Furthermore, immunoblotting results indicated that 48 hours of 2.5 μM mercaptopurine exposure stimulated apoptosis in LS180 KD cells (fold change 3.25 ± 0.42, P = 0.050) compared to the untreated samples, indicating a higher apoptotic level in LS180 KD cells at this time point.

Because the disruption of the mitochondrial membrane is one of the crucial steps of apoptosis activation by both intrinsic and extrinsic pathways, DiOC6 assay was performed to evaluate the percentage of mitochondrial membrane depolarization under basal condition and after 24, 48 and 72 hours of mercaptopurine treatment. Moreover, cells exposed to 5 μM doxorubicin, an apoptosis inducer, were used as positive control. Compared to untreated cells, a significant reduction in the percentage of mitochondrial membrane potential after 5 μM doxorubicin exposure for 24, 48 and 72 hours was observed, both in LS180 MOCK (untreated cell vs 5 μM doxorubicin: -23.67%, P = 0.035 for 24 hours, -34.34%, P < 0.0001 for 48 hours, -41.13%, P < 0.0001 for 72 hours, figure 15c) and LS180 KD cells (untreated cell vs 5 μM doxorubicin: -25.39%, P = 0.041 for 24 hours, -37.72%, P < 0.0001 for 48 hours, -42.46%, P < 0.0001 for 72 hours, figure 15c), confirming that doxorubicin exposure induces apoptosis and is a good positive control. Interestingly, after 72 hours of mercaptopurine treatment, the percentage of the mitochondrial membrane potential was reduced in LS180 KD exposed to this drug (untreated cells vs 1.25 μM: -15.95%, P = 0.026; untreated cells vs 2.5 μM: -26.42%, P < 0.0001, figure 15c), indicating increased apoptotic levels after mercaptopurine exposure. The percentage of the mitochondrial membrane potential in LS180 KD cells was lower compared to MOCK control cells after 72 hours of 2.5 μM mercaptopurine exposure (MOCK vs KD: -19.69%, P = 0.0012, figure 15c), further supporting the presence of higher apoptosis in the intestinal LS180 KD cells after mercaptopurine exposure.

Taken together with the mercaptopurine cytotoxicity results on the intestinal LS180 cells, these results indicate a possible contribution of apoptosis in mercaptopurine induced cellular death, which is more evident in LS180 KD cells.

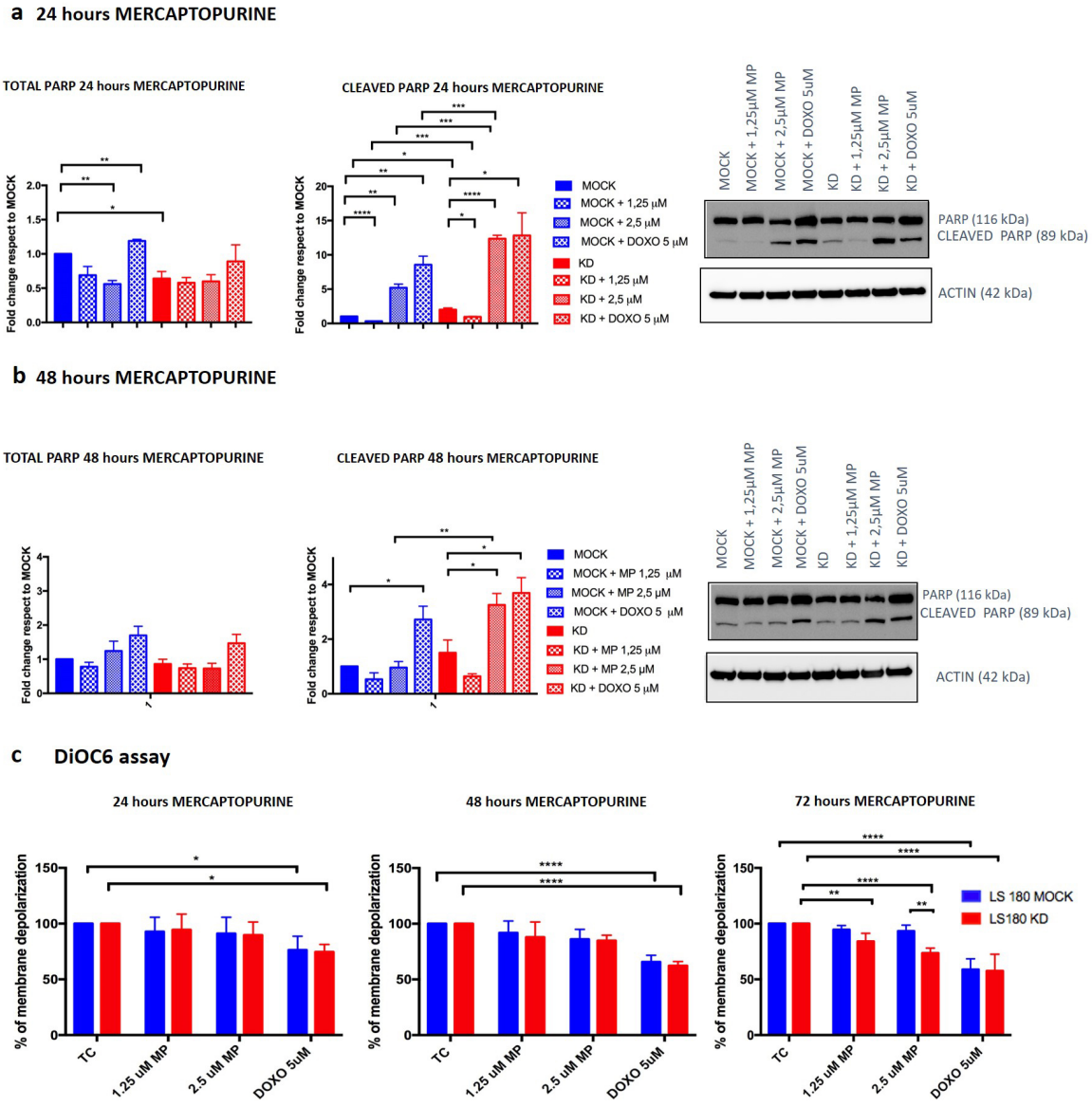


***Figure 15: the effect of PACSIN2 KD and mercaptopurine treatment on autophagy.*** *A) Immunoblotting results of total and cleaved PARP1 in LS180 cell lines under basal condition or after 24 hours of treatment with 1.25 µM, 2.5 µM mercaptopurine or 5 µM doxorubicin showed that drugs induced apoptosis in both cell lines; interestingly, this increase was higher in presence of PACSIN2 KD. B) Immunoblotting results of total and cleaved PARP1 in LS180 cell lines under basal condition or after 48 hours of 1.25 µM, 2.5 µM mercaptopurine or 24 hours of 5 µM doxorubicin treatment in LS180 cell lines showed that drug exposure induces apoptosis, especially in cells with PACSIN2 KD. Western blot experiments were performed using 10 µg of cell lysate. C) DiOC6 assay results showed the percentage of the mitochondrial membrane polarization under basal condition and after 24, 48 or 72 hours of mercaptopurine exposure; 24 hours of 5 µM doxorubicin treatment was used as positive control. After treatment, cells with PACSIN2 KD showed a lower mitochondrial membrane depolarization, supporting the immunoblotting evidences about the potential role of mercaptopurine as apoptotic inducer. All experiments were performed at least three times. * p-value ≤ 0.05, ** p-value ≤ 0.01, *** p-value ≤ 0.001, **** p-value ≤ 0.0001.*

## 11. *PACSIN2* KD did not impact on thiopurine metabolites TGN and MMPN concentrations in LS180 cells

The amount of cellular thiopurines metabolites TGN and MMPN was quantified by HPLC-UV after treating cells with 2.5 µM mercaptopurine for 24 and 48 hours.

The *PACSIN2* KD did not impact in a significant way on the amount of TGN active metabolites (figure 16a) and MMPN metabolites (figure 16b) in drug-treated cells, regardless of the exposure time. Indeed, the level of TGN remained stable over drug exposure time, although a non-significant reduction was observed at 48 hours comparted to 24 hours, whereas MMPN were reduced after prolonged exposure. No statistical difference in MMPN levels was detected between LS180 MOCK and KD cells after 24 and 48 hours of mercaptopurine exposure.

Taken together, these results showed that *PACSIN2* KD did not impact in a significant way on the amount of thiopurine metabolites, indicating that PACSIN2 is not able to affect thiopurine pharmacokinetics.

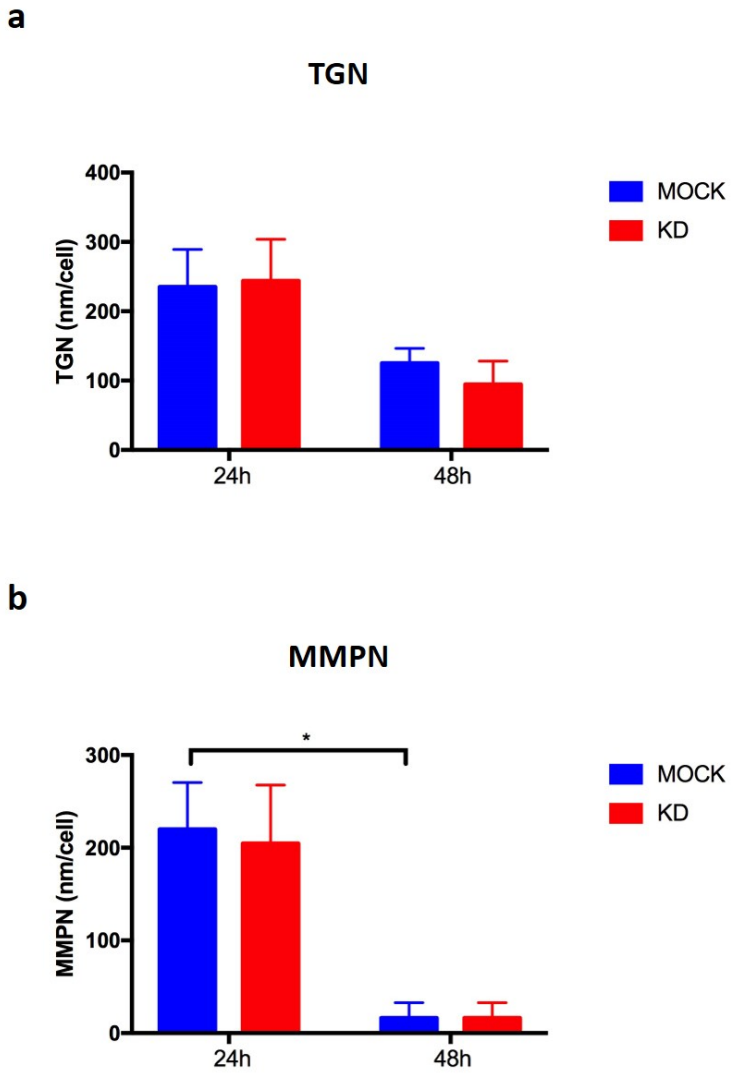


***Figure 16: the amount of thiopurine metabolites after 24 hours and 48 hours of mercaptopurine exposure In LS180 cells****. A) The timing of mercaptopurine exposure and the presence of PACSIN2 KD did not affect TGN levels. B) Both 24 hours and 48 hours of mercaptopurine exposure reduced MMPN levels in both LS180 MOCK and LS180 KD cells, but this difference reached a statistically significant difference only in LS180 MOCK cells (n=3, P = 0.037, 2-way ANOVA). Moreover, the presence of PACSIN2 KD did not impact on MMPN levels. All experiments were performed at least three times. * p-value ≤ 0.05.*

## 12. PACSIN2 modulated TPMT activity through a molecular mechanism different from autophagy

In order to investigate the possible correlation between PACSIN2, autophagy and TPMT levels, western blot analyses were performed to assess TPMT and LC3-II levels under basal condition and after exposure to 30 μM of chloroquine in NALM6 cells.

As stated previously, the overexpression of TPMT in NALM6 *1 and NALM6 KD*1 resulted in the presence of a double band for TPMT: one for the endogenous protein (36 kDa), observable also in NALM6 MOCK and NALM6 KD cells and another band for the exogenous TPMT isoform (DDK-TPMT, 38 kDa) (Figure 17a) The immunoblotting results showed a higher amount of total TPMT in NALM6*1 compared to MOCK control cells (fold change 2.6 ± 0.5, P = 0.031). NALM6 KD*1 showed a lower amount of the overexpressed isoform of TPMT compared to NALM6 *1 (fold change 0.56 ± 0.17, P = .021), indicating that PACSIN2 could modulate TPMT expression levels only in a supra-physiological condition. (Figure 17a) Moreover, these immunoblotting results showed no difference in TPMT amount in NALM6 cell after chloroquine exposure. (Figure 17a)

It seems that the overexpression of TPMT increased LC3-II levels in NALM6*1 cells compared to MOCK and was further increased in NALM6 KD*1 cells, indicating a similar trend to the one detected between NALM6 MOCK and NALM6 KD cells; however, these results suffered of high intra-experimental variability and did not reach a statistically significance. (Figure 17b).

Taken together, these results did not find a correlation between autophagy and TPMT levels, suggesting that modulation of autophagy is not the molecular mechanism at the basis of PACSIN2 modulation of TPMT activity.

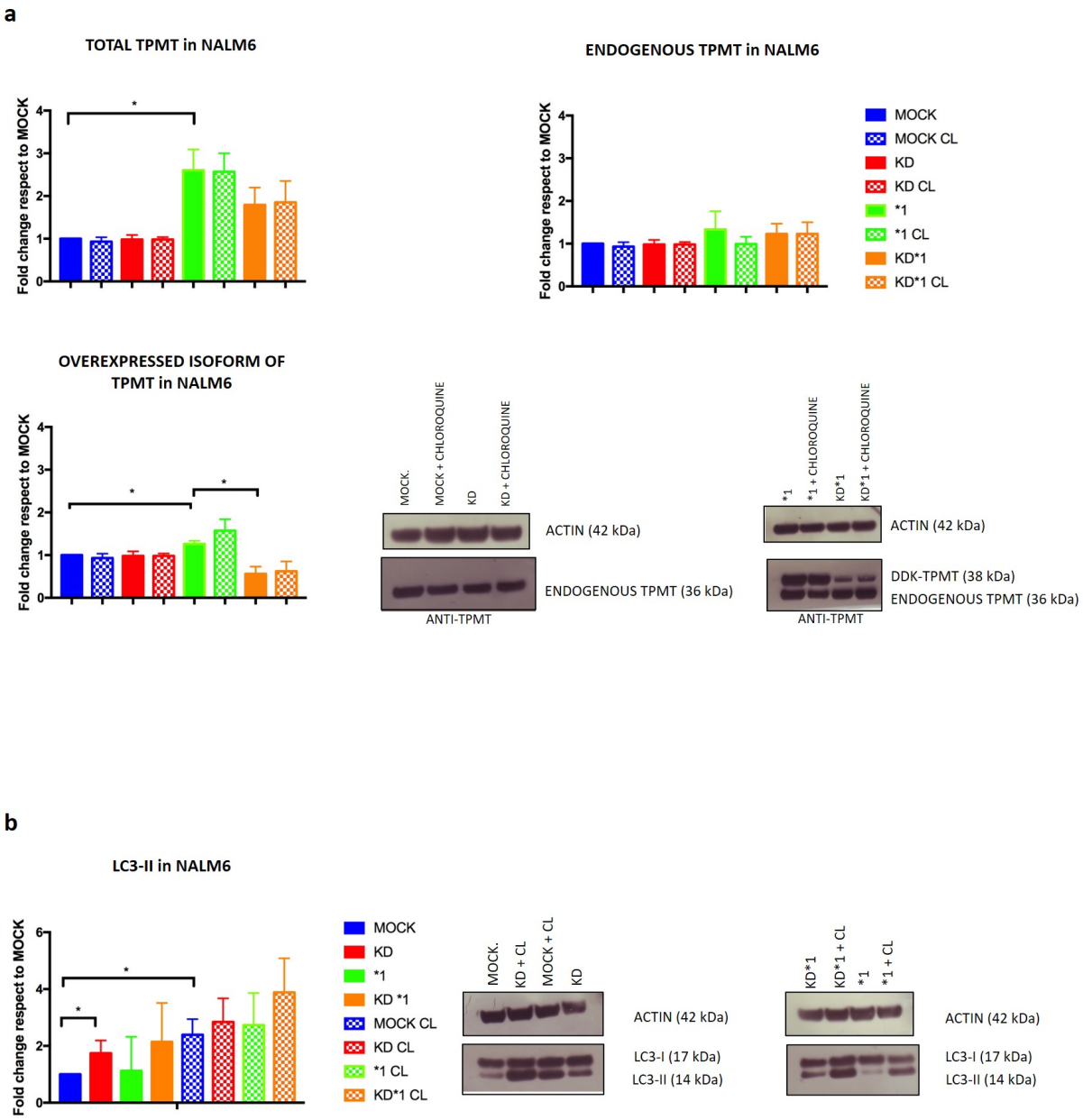


***Figure 17: TPMT and LC3 levels in NALM6****. A) PACSIN2 KD reduces only the amount of the overexpressed isoform of TPMT in NALM6 cell; chloroquine exposure did not impact on TPMT levels. B) TPMT overexpression and the presence of both TPMT overexpression and PACSIN2 KD did not impact in a significant way on LC3-II levels in NALM6 cell lines. Immunoblottings were performed using 10 µg of cell lysate.*

# DISCUSSION

PACSINs are membrane proteins involved in multiple biological processes. (Dumont & Lehtonen, 2022) They exert their function mainly through protein–protein interactions with different substrates, such as Arp2/3, dynamin and Rac-1. (de Kreuk et al., 2011) Previous data showed that PACSINs play different roles in cells, such as endocytosis modulation (de Kreuk et al., 2012) and membrane tubulation. PACSIN2 showed a homology sequence with PACSIN1, which was implicated in autophagy regulation in the human breast carcinoma MCF-7 cells. (Szyniarowski et al., 2011) In order to evaluate the possible role of PACSIN2 in autophagy, the impact of *PACSIN2* KD on the autophagic markers LC3 and SQSTM1/P62 was evaluated in different *in vitro* models representative of the lymphoid and intestinal tissues. The inverse correlation found between PACSIN2 amount and autophagy levels suggested that PACSIN2 could be considered an autophagy inhibitor. A previous study with a similar experimental scheme was used to investigate the possible role of the ER membrane protein BAP31 as autophagic modulator on osteosarcoma U2OS cells and MEF cells transfected with small interfering RNA (siRNA) for silencing *BAP31* and showed increased LC3-II protein amount in *BAP31* KD cells, concluding that BAP31 is a negative autophagy regulator. (Machihara & Namba, 2019) Interestingly, the inverse correlation between PACSIN2 amount and autophagy levels found in *in vitro* models was confirmed in colon samples of IBD pediatric patients; in particular, PACSIN2 gene and protein concentrations were decreased in presence of higher autophagy in inflamed colon samples, supporting the above-mentioned hypothesis of PACSIN2 involvement in autophagy arising by the analysis on our NALM6 and LS180 cell models. Consistently, a recent study identified a higher amount of the autophagy protein ATG10 in colon biopsies of IBD patients compared to healthy donors. (Abbasi Teshnizi et al., 2021) In order to clarify in which step of autophagy PACSIN2 exerts its function, both LC3 and SQSTM1/P62 levels were evaluated after chloroquine exposure, that impairs the last part of the autophagic flux, blocking autophagosomes fusion with lysosomes. (Yoshii & Mizushima, 2017) (Jiang & Mizushima, 2015) Interestingly, autophagy was further increased after chloroquine exposure in cells with *PACSIN2* KD, suggesting that PACSIN2 affects the beginning of the autophagic flux and does not cause a defect in lysosomal degradation. (Yoshii & Mizushima, 2017) In the above-mentioned study on BAP31, Machihara and collaborators found a similar result after exposure of U2OS and MEF cells to bafilomycin A1, a substance presenting the same mechanism of action of chloroquine (autophagosome-lysosome fusion blockage) (Fedele & Proud, 2020), indicating that BAP31 modulates negatively autophagy acting in the first phases of the autophagic flux, impairing

autophagosomes formation. In particular, they identified a further increase of LC3-II after bafilomycin A1 treatment in cells without BAP31. (Machihara & Namba, 2019) Taken together these evidences show for the first time the involvement of PACSIN2 in the autophagy machinery, demonstrating that PACSIN2 is a negative modulator of autophagy and is implicated in the early phase of this cellular mechanism.

PACSIN2 protein shows different interacting region domains, responsible for a physical interaction with other proteins, such as Rac-1, Cobll1 and SH3BP1, in order to modulate different cellular biological processes. (de Kreuk et al., 2011) (Park et al., 2022) In particular, PACSIN2 regulates cell stiffness and migration binding Rac-1 (de Kreuk et al., 2011), whereas PACSIN2 physical interaction with Cobll1 and SH3BP1 impact on drug sensitivity in chronic myeloid leukemia cell lines (K562) and control embryonic myeloid development in zebrafish, suggesting a role of PACSIN2 in the regulation of hematopoiesis in vertebrates. (Park et al., 2022) Different autophagy modulators exert their function interacting with LC3, a key autophagy protein involved in elongation and maturation of autophagosomes. (Birgisdottir et al., 2013) (Mizushima et al., 2010) (Chun & Kim, 2018). Different receptors involved in autophagy modulation, such as NBR1, FYCO1, NIX, PLEKHM1 and JIP1 present a LIR domain, through which they exert their function on autophagy. (Rozenknop et al., 2011) (Olsvik et al., 2015) (Novak et al., 2010) (McEwan et al., 2015) (Fu et al., 2014) The results obtained from *in silico* analysis performed using iLIR database identified a LIR motif in the PACSIN2 N-terminal protein sequence and, interestingly, this domain was demonstrated to be responsible for a protein-protein interaction between PACSIN2 and LC3. We therefore provided experimental evidence of the physical interaction between PACSIN2 and LC3-II that could represent the molecular mechanism used by PACSIN2 to inhibit autophagy. Consistently, Pankiv and collaborators found a LIR domain on the SQSTM1/P62 primary amino acidic sequence and demonstrated that it is fundamental for the physical binding with LC3. (Pankiv et al., 2007) In particular, the N-terminal region of the PACSIN2 protein contains an evolutionarily conserved motif (D-D-W-T-H-L), presenting an aromatic amino acid in the central position and an aliphatic amino acid in the last position of the motif. (Birgisdottir et al., 2013)

Autophagy is considered a cellular survival mechanism in response to different stress sources, such as ER stress (Ogata et al., 2006); however, in presence of elevated stress conditions, autophagy may contribute to cell death. (Liu et al., 2017) In this study, NALM6 KD cells presented higher sensitivity to the ER-stress inducer tunicamycin, indicating that PACSIN2 loss could worsen the ER-stressing condition of tunicamycin activating autophagy. The presence of unfolded proteins stimulates the ER stress response, activating the unfolded protein response (UPR) pathway, leading to mTORC1 activation and autophagy inhibition with consequent SQSTM1/P62 accumulation. (Guha et al., 2017)

A previous study performed on wild type (SQSTM1/P62$^{+/+}$) and SQSTM1/P62-deficient (SQSTM1/P62$^{-/-}$) MEF cells exposed to tunicamycin showed higher apoptosis after SQSTM1/depletion. (Park et al., 2016) Consistently, the immunoblotting for SQSTM1/P62 showed higher autophagy levels in NALM6 KD cells, which were associated to a lower SQSTM1/P62 amount and to an increased tunicamycin sensitivity.

The possible impact of both *PACSIN2* KD and autophagy on TPMT amount was evaluated in this study, showing that *PACSIN2* KD did not affect the endogenous TPMT levels, but NALM6 KD*1 cells showed a lower amount of the overexpressed isoform of TPMT. Moreover, TPMT amount was not affected by chloroquine exposure and the presence of TPMT*1 overexpression did not impact in a significant way to cell autophagy levels, indicating other possible mechanisms at the basis of cellular TPMT degradation; indeed, previous results demonstrated that TPMT could be targeted for degradation by the proteasome rather than autophagy. (Li et al., 2008) (Tai et al., 1999) Therefore, other molecular mechanisms must be considered to explain the influence of PACSIN2 on TPMT activity, such as a direct modulation of *TPMT* mRNA levels by *PACSIN2*, consistent with a previous result of Stocco and colleagues that found a reduction of both PACSIN2 protein and mRNA levels in NALM6 KD cells, presenting lower TPMT expression and activity levels. (Stocco et al., 2012)

The cytotoxicity results for mercaptopurine indicated that TPMT overexpression in NALM6 cells increased significantly cell mercaptopurine sensitivity, consistent with a previous study, that demonstrated a higher thiopurine sensitivity in NALM6*1 cells compared to MOCK related to the supraphysiological accumulation of methylated metabolites, that occurs *in vitro* upon TPMT overexpression. (Dervieux et al., 2001) Interestingly, the presence of *PACSIN2* KD was able to rescue this effect, supporting the hypothesis of PACSIN2 influence on TPMT activity, previously demonstrated both in this cell lines and in ALL pediatric patients. (Stocco et al., 2012) Moreover, the possible impact of *PACSIN2* KD on the amount of thiopurin metabolites (TGN and MMPN) was evaluated by HPLC-UV, showing that the *PACSIN2* KD did not affect thiopurine metabolites levels, suggesting that PACSIN2 is not able to affect thiopurine pharmacokinetics but rather act on their pharmacodynamics.

The cytotoxicity results for mercaptopurine showed that *PACSIN2* KD increased significantly the drug sensitivity only in the intestinal LS180 cell and not in leukemic NALM6 cells, leading to hypothesize a tissue specific role of PACSIN2 in the intestine. Interestingly, the *PACSIN2* KD increased also thioguanine cell sensitivity in LS180 cells, whereas no differences were detected in cell sensitivity to 5-fluorouracil, a non-thiopurines antimetabolite, leading to hypothesize a role of PACSIN2 in the specific cytotoxic mechanisms of thiopurines. To test the cytotoxicity of a non-thiopurine antimetabolite, t5-fluorouracil was chosen bon the basis of previous data of the Human

Protein Atlas tool indicating that lower PACSIN2 levels were associated with a reduced survival of colorectal adenocarcinoma patients exposed to 5-fluorouracil. (www.proteinatlas.org) (Vodenkova et al., 2020). Taken together these evidences suggested a possible tissue specific role of PACSIN2 in the intestine after thiopurine exposure through unknown mechanisms. To further investigate this hypothesis, autophagy and apoptosis levels were evaluated in intestinal cell lines after mercaptopurine exposure, showing that mercaptopurine treatment was able to increase apoptosis and to reduce autophagy. This result on autophagy is in contrast with a previous report that found higher LC3-II levels after mercaptopurine treatment on other stabilized intestinal cell lines (HT29 cells). However, Chaabane and collaborators evaluated autophagy after cell exposure to higher concentrations of mercaptopurine (50 μM mercaptopurine for 24 hours), compared to those used in this study (1.25 μM and 2.5 μM for 24 hour and 48 hours). Moreover, Chaabane and collegues analyzed cells after a longer time of drug exposure (72 hours) and after replacement of drug with fresh medium, that could be a source of energy and may stimulate the activation of survival mechanisms, such as autophagy.(Chaabane & Appell, 2016)

The results obtained in this study indicated that mercaptopurine treatment reduces autophagy in a dose dependent way and interestingly, *PACSIN2* KD counteracts this effect; LS180 KD cells showed also higher apoptosis compared to control cells, indicating that the higher autophagy levels present in these cells were able to promote apoptosis after mercaptopurine exposure. These evidences were consistent with the cytotoxicity results that indicated a higher mercaptopurine sensitivity in cells with *PACSIN2* KD after 72 hours of drug exposure, and were also consistent with DiOC6 assay results, which indicated that 72 hours of mercaptopurine exposure stimulated apoptosis in the LS180 KD cells. Taken together, these observations confirm the role of PACSIN2 as a regulator of autophagy and suggest that higher autophagy levels are associated with mercaptopurine induced apoptosis in the intestinal LS180 cells. Similar results, indicating a correlation between higher autophagy levels with apoptosis induction was found in the in the human colorectal cancer cells HCT116; in particular, authors found that the antitumor zoledronic acid derivative $M_4IDP_4$ stimulated autophagy in a significant way, leading to increased ROS production and ER stress and promoting apoptosis. (Peng et al., 2017) Consistently, Wang et al. found that HeLa cells exposure to the antimalarial dihydroartemisinin, an agent able to simulate free radical production, increased both autophagic and apoptotic protein levels, leading to cell death, and DNA double-strand breaks damage generation. (Wang et al., 2019) A correlation between autophagy and apoptosis was identified by different studies, however the molecular mechanism at the basis of this interconnection remains not completely understood and different studies showed contrasting results, indicating that the cell type and drug treatment conditions could impact on the balance between autophagy and apoptosis. (Xie et al., 2020)

The interconnection may occur at different stages and may be exerted by different autophagic and apoptotic molecules, such as Beclin-1, Bcl-2, PINK1 and SQSTM1/P62 (Wang et al., 2019) (Djavaheri-Mergny et al., 2010) (Zhang et al., 2018) (Zhu et al., 2021). Zhu and collaborators showed that the antitumor drug neferine, a P-glicoprotein inhibitor, was able to stimulate apoptosis inhibiting autophagy, through SQSTM1/P62 accumulation in the head and neck squamous carcinoma cells (HNSCC). (Zhu et al., 2021) Also ROS may exert an important role in this crosstalk, leading to autophagy inhibition and apoptosis stimulation. (Dang et al., 2015) Interestingly, Chaabane and collaborators demonstrated that thiopurines disrupt mitochondrial membrane potential increasing ROS production and stimulating apoptosis. (Chaabane & Appell, 2016) The results of this thesis demonstrated that also PACSIN2 influences mercaptopurine effects on autophagy and apoptosis in intestinal cell models, supporting the role of PACSIN2 on mercaptopurine response and also on autophagy regulation. However, the specific molecular mechanism of PACSIN2 in this interplay remains not clear and further investigations are needed to clarify the molecular mechanisms at the basis of PACSIN2 role in the crosstalk between autophagy and apoptosis.

# CONCLUSION AND FUTURE AIMS

Taken together, these findings demonstrate a clear role of PACSIN2 as an inhibitor of autophagy, probably through the inhibition of autophagosomes formation by a physical interaction with LC3-II that is mediated by a LIR motif present in the PACSIN2 sequence.

*PACSIN2* KD impact mercaptopurine cytotoxic effect on cells of intestinal origin but not on lymphoid cells, suggesting a possible tissue specific role of PACSIN2 in the intestine and interestingly, further investigations demonstrated also a possible role of PACSIN2 in the interplay between autophagy and apoptosis after mercaptopurine exposure in the intestinal cells. Moreover, our results indicated that PACSIN2 is not able to affect thiopurine pharmacokinetics. Furthermore, the immunoblotting results for TPMT and LC3 suggested that autophagy is not the molecular mechanism at the basis of PACSIN2 impact on TPMT activity.

Because the results of previous studies demonstrated an involvement of *PACSIN2* rs2413739 variant on TPMT activity and thiopurine-related toxicity development, it will be interesting to generate an *in vitro* intestinal model of the rs2413739 variant, that has been associated to a reduced TPMT activity and expression levels, in order to deeply investigate the possible impact of this polymorphism in the intestine.

# REFERENCES


Abada, A., Levin-Zaidman, S., Porat, Z., Dadosh, T., & Elazar, Z. (2017). SNARE priming is essential for maturation of autophagosomes but not for their formation. *Proc Natl Acad Sci U S A*, *114*(48), 12749-12754. https://doi.org/10.1073/pnas.1705572114

Abbasi Teshnizi, F., Kazemipour, N., Nazifi, S., Bagheri Lankarani, K., Sepehrimanesh, M., & Razeghian Jahromi, I. (2021). A study on the potential role of autophagy-related protein 10 as a biomarker for ulcerative colitis. *Physiol Rep*, *9*(7), e14825. https://doi.org/10.14814/phy2.14825

Adam de Beaumais, T., Fakhoury, M., Medard, Y., Azougagh, S., Zhang, D., Yakouben, K., & Jacqz-Aigrain, E. (2011). Determinants of mercaptopurine toxicity in paediatric acute lymphoblastic leukemia maintenance therapy. *Br J Clin Pharmacol*, *71*(4), 575-584. https://doi.org/10.1111/j.1365-2125.2010.03867.x

Adehin, A., & Bolaji, O. O. (2018). Thiopurine S-methyltransferase activity in Nigerians: phenotypes and activity reference values. *BMC Res Notes*, *11*(1), 129. https://doi.org/10.1186/s13104-018-3237-5

Alemu, E. A., Lamark, T., Torgersen, K. M., Birgisdottir, A. B., Larsen, K. B., Jain, A., . . . Johansen, T. (2012). ATG8 family proteins act as scaffolds for assembly of the ULK complex: sequence requirements for LC3-interacting region (LIR) motifs. *J Biol Chem*, *287*(47), 39275-39290. https://doi.org/10.1074/jbc.M112.378109

Birgisdottir, Å., Lamark, T., & Johansen, T. (2013). The LIR motif - crucial for selective autophagy. *J Cell Sci*, *126*(Pt 15), 3237-3247. https://doi.org/10.1242/jcs.126128

Borutaite, V. (2010). Mitochondria as decision-makers in cell death. *Environ Mol Mutagen*, *51*(5), 406-416. https://doi.org/10.1002/em.20564

Bouchard, V. J., Rouleau, M., & Poirier, G. G. (2003). PARP-1, a determinant of cell survival in response to DNA damage. *Exp Hematol*, *31*(6), 446-454. https://doi.org/10.1016/s0301-472x(03)00083-3

Bratton, S. B., & Salvesen, G. S. (2010). Regulation of the Apaf-1-caspase-9 apoptosome. *J Cell Sci*, *123*(Pt 19), 3209-3214. https://doi.org/10.1242/jcs.073643

Broekman, M. M. T. J., Coenen, M. J. H., Wanten, G. J., van Marrewijk, C. J., Klungel, O. H., Verbeek, A. L. M., . . . de Jong, D. J. (2017). Risk factors for thiopurine-induced myelosuppression and

infections in inflammatory bowel disease patients with a normal TPMT genotype. *Aliment Pharmacol Ther*, *46*(10), 953-963. https://doi.org/10.1111/apt.14323

Cara, C. J., Pena, A. S., Sans, M., Rodrigo, L., Guerrero-Esteo, M., Hinojosa, J., . . . Guijarro, L. G. (2004). Reviewing the mechanism of action of thiopurine drugs: towards a new paradigm in clinical practice. *Med Sci Monit*, *10*(11), RA247-254.

Chaabane, W., & Appell, M. L. (2016). Interconnections between apoptotic and autophagic pathways during thiopurine-induced toxicity in cancer cells: the role of reactive oxygen species. *Oncotarget*, *7*(46), 75616-75634. https://doi.org/10.18632/oncotarget.12313

Choi, R., Chun, M. R., Park, J., Lee, J. W., Ju, H. Y., Cho, H. W., . . . Lee, S. Y. (2021). Quantification of Thioguanine in DNA Using Liquid Chromatography-Tandem Mass Spectrometry for Routine Thiopurine Drug Monitoring in Patients With Pediatric Acute Lymphoblastic Leukemia. *Ann Lab Med*, *41*(2), 145-154. https://doi.org/10.3343/alm.2021.41.2.145

Choi, R., Sohn, I., Kim, M. J., Woo, H. I., Lee, J. W., Ma, Y., . . . Lee, S. Y. (2019). Pathway genes and metabolites in thiopurine therapy in Korean children with acute lymphoblastic leukaemia. *Br J Clin Pharmacol*, *85*(7), 1585-1597. https://doi.org/10.1111/bcp.13943

Chun, Y., & Kim, J. (2018). Autophagy: An Essential Degradation Program for Cellular Homeostasis and Life. *Cells*, *7*(12). https://doi.org/10.3390/cells7120278

Conter, V., Bartram, C. R., Valsecchi, M. G., Schrauder, A., Panzer-Grümayer, R., Möricke, A., . . . Schrappe, M. (2010). Molecular response to treatment redefines all prognostic factors in children and adolescents with B-cell precursor acute lymphoblastic leukemia: results in 3184 patients of the AIEOP-BFM ALL 2000 study. *Blood*, *115*(16), 3206-3214. https://doi.org/10.1182/blood-2009-10-248146

Dang, S., Yu, Z. M., Zhang, C. Y., Zheng, J., Li, K. L., Wu, Y., . . . Wang, R. X. (2015). Autophagy promotes apoptosis of mesenchymal stem cells under inflammatory microenvironment. *Stem Cell Res Ther*, *6*, 247. https://doi.org/10.1186/s13287-015-0245-4

Daumke, O., Roux, A., & Haucke, V. (2014). BAR domain scaffolds in dynamin-mediated membrane fission. *Cell*, *156*(5), 882-892. https://doi.org/10.1016/j.cell.2014.02.017

de Kreuk, B. J., Anthony, E. C., Geerts, D., & Hordijk, P. L. (2012). The F-BAR protein PACSIN2 regulates epidermal growth factor receptor internalization. *J Biol Chem*, *287*(52), 43438-43453. https://doi.org/10.1074/jbc.M112.391078

de Kreuk, B. J., Nethe, M., Fernandez-Borja, M., Anthony, E. C., Hensbergen, P. J., Deelder, A. M., . . . Hordijk, P. L. (2011). The F-BAR domain protein PACSIN2 associates with Rac1 and regulates

cell spreading and migration. *J Cell Sci*, *124*(Pt 14), 2375-2388. https://doi.org/10.1242/jcs.080630

Derijks, L. J. J., Wong, D. R., Hommes, D. W., & van Bodegraven, A. A. (2018). Clinical Pharmacokinetic and Pharmacodynamic Considerations in the Treatment of Inflammatory Bowel Disease. *Clin Pharmacokinet*, *57*(9), 1075-1106. https://doi.org/10.1007/s40262-018-0639-4

Dervieux, T., Blanco, J. G., Krynetski, E. Y., Vanin, E. F., Roussel, M. F., & Relling, M. V. (2001). Differing contribution of thiopurine methyltransferase to mercaptopurine versus thioguanine effects in human leukemic cells. *Cancer Res*, *61*(15), 5810-5816.

Dervieux, T., & Boulieu, R. (1998). Simultaneous determination of 6-thioguanine and methyl 6-mercaptopurine nucleotides of azathioprine in red blood cells by HPLC. *Clin Chem*, *44*(3), 551-555.

Djavaheri-Mergny, M., Maiuri, M. C., & Kroemer, G. (2010). Cross talk between apoptosis and autophagy by caspase-mediated cleavage of Beclin 1. *Oncogene*, *29*(12), 1717-1719. https://doi.org/10.1038/onc.2009.519

Dubinsky, M. C., Lamothe, S., Yang, H. Y., Targan, S. R., Sinnett, D., Théorêt, Y., & Seidman, E. G. (2000). Pharmacogenomics and metabolite measurement for 6-mercaptopurine therapy in inflammatory bowel disease. *Gastroenterology*, *118*(4), 705-713. https://doi.org/10.1016/s0016-5085(00)70140-5

Dumont, V., & Lehtonen, S. (2022). PACSIN proteins in vivo: Roles in development and physiology. *Acta Physiol (Oxf)*, *234*(3), e13783. https://doi.org/10.1111/apha.13783

Edinger, A. L., & Thompson, C. B. (2004). Death by design: apoptosis, necrosis and autophagy. *Curr Opin Cell Biol*, *16*(6), 663-669. https://doi.org/10.1016/j.ceb.2004.09.011

Eklund, B. I., Moberg, M., Bergquist, J., & Mannervik, B. (2006). Divergent activities of human glutathione transferases in the bioactivation of azathioprine. *Mol Pharmacol*, *70*(2), 747-754. https://doi.org/10.1124/mol.106.025288

Elmore, S. (2007). Apoptosis: a review of programmed cell death. *Toxicol Pathol*, *35*(4), 495-516. https://doi.org/10.1080/01926230701320337

Erb, N., Harms, D. O., & Janka-Schaub, G. (1998). Pharmacokinetics and metabolism of thiopurines in children with acute lymphoblastic leukemia receiving 6-thioguanine versus 6-mercaptopurine. *Cancer Chemother Pharmacol*, *42*(4), 266-272. https://doi.org/10.1007/s002800050816

Eskelinen, E. L., Illert, A. L., Tanaka, Y., Schwarzmann, G., Blanz, J., Von Figura, K., & Saftig, P. (2002). Role of LAMP-2 in lysosome biogenesis and autophagy. *Mol Biol Cell*, *13*(9), 3355-3368. https://doi.org/10.1091/mbc.e02-02-0114

Fedele, A. O., & Proud, C. G. (2020). Chloroquine and bafilomycin A mimic lysosomal storage disorders and impair mTORC1 signalling. *Biosci Rep*, *40*(4). https://doi.org/10.1042/BSR20200905

Franca, R., Braidotti, S., Stocco, G., & Decorti, G. (2021). Understanding thiopurine methyltransferase polymorphisms for the targeted treatment of hematologic malignancies. *Expert Opin Drug Metab Toxicol*, *17*(10), 1187-1198. https://doi.org/10.1080/17425255.2021.1974398

Franca, R., Stocco, G., Favretto, D., Giurici, N., Del Rizzo, I., Locatelli, F., . . . Rabusin, M. (2020). PACSIN2 rs2413739 influence on thiopurine pharmacokinetics: validation studies in pediatric patients. *Pharmacogenomics J*, *20*(3), 415-425. https://doi.org/10.1038/s41397-019-0130-0

Franca, R., Zudeh, G., Lucafò, M., Rabusin, M., Decorti, G., & Stocco, G. (2021). Genome wide association studies for treatment-related adverse effects of pediatric acute lymphoblastic leukemia. *WIREs Mech Dis*, *13*(3), e1509. https://doi.org/10.1002/wsbm.1509

Franca, R., Zudeh, G., Pagarin, S., Rabusin, M., Lucafò, M., Stocco, G., & Decorti, G. (2019). Pharmacogenetics of thiopurines. *Cancer Drug Resist*, *2*(2), 256-270. https://doi.org/10.20517/cdr.2019.004

Fu, M. M., Nirschl, J. J., & Holzbaur, E. L. F. (2014). LC3 binding to the scaffolding protein JIP1 regulates processive dynein-driven transport of autophagosomes. *Dev Cell*, *29*(5), 577-590. https://doi.org/10.1016/j.devcel.2014.04.015

Gisbert, J. P., & Gomollón, F. (2008). Thiopurine-induced myelotoxicity in patients with inflammatory bowel disease: a review. *Am J Gastroenterol*, *103*(7), 1783-1800. https://doi.org/10.1111/j.1572-0241.2008.01848.x

Grimm-Günter, E. M., Milbrandt, M., Merkl, B., Paulsson, M., & Plomann, M. (2008). PACSIN proteins bind tubulin and promote microtubule assembly. *Exp Cell Res*, *314*(10), 1991-2003. https://doi.org/10.1016/j.yexcr.2008.03.015

Grumati, P., & Dikic, I. (2018). Ubiquitin signaling and autophagy. *J Biol Chem*, *293*(15), 5404-5413. https://doi.org/10.1074/jbc.TM117.000117

Gubas, A., & Dikic, I. (2022). A guide to the regulation of selective autophagy receptors. *FEBS J*, *289*(1), 75-89. https://doi.org/10.1111/febs.15824

Guha, P., Kaptan, E., Gade, P., Kalvakolanu, D. V., & Ahmed, H. (2017). Tunicamycin induced endoplasmic reticulum stress promotes apoptosis of prostate cancer cells by activating mTORC1. *Oncotarget*, *8*(40), 68191-68207. https://doi.org/10.18632/oncotarget.19277

Harvey, N. L., & Kumar, S. (1998). The role of caspases in apoptosis. *Adv Biochem Eng Biotechnol*, *62*, 107-128. https://doi.org/10.1007/BFb0102307

Inaba, H., & Pui, C. H. (2019). Immunotherapy in pediatric acute lymphoblastic leukemia. *Cancer Metastasis Rev*, *38*(4), 595-610. https://doi.org/10.1007/s10555-019-09834-0

Jacomin, A. C., Samavedam, S., Promponas, V., & Nezis, I. P. (2016). iLIR database: A web resource for LIR motif-containing proteins in eukaryotes. *Autophagy*, *12*(10), 1945-1953. https://doi.org/10.1080/15548627.2016.1207016

Jiang, P., & Mizushima, N. (2015). LC3- and p62-based biochemical methods for the analysis of autophagy progression in mammalian cells. *Methods*, *75*, 13-18. https://doi.org/10.1016/j.ymeth.2014.11.021

Karanasios, E., Walker, S. A., Okkenhaug, H., Manifava, M., Hummel, E., Zimmermann, H., . . . Ktistakis, N. T. (2016). Autophagy initiation by ULK complex assembly on ER tubulovesicular regions marked by ATG9 vesicles. *Nat Commun*, *7*, 12420. https://doi.org/10.1038/ncomms12420

Karim, H., Appell, M. L., & Fotoohi, A. (2013). Comparison of three methods for measuring thiopurine methyltransferase activity in red blood cells and human leukemia cells. *J Chromatogr B Analyt Technol Biomed Life Sci*, *939*, 80-85. https://doi.org/10.1016/j.jchromb.2013.08.036

Kaushik, S., & Cuervo, A. M. (2012). Chaperone-mediated autophagy: a unique way to enter the lysosome world. *Trends Cell Biol*, *22*(8), 407-417. https://doi.org/10.1016/j.tcb.2012.05.006

Kessels, M. M., & Qualmann, B. (2002). Syndapins integrate N-WASP in receptor-mediated endocytosis. *EMBO J*, *21*(22), 6083-6094. https://doi.org/10.1093/emboj/cdf604

Khaeso, K., Udayachalerm, S., Komvilaisak, P., Chainansamit, S. O., Suwannaying, K., Laoaroon, N., . . . Chaiyakunapruk, N. (2021). Meta-Analysis of. *Front Pharmacol*, *12*, 784712. https://doi.org/10.3389/fphar.2021.784712

Kim, M. Y., Zhang, T., & Kraus, W. L. (2005). Poly(ADP-ribosyl)ation by PARP-1: 'PAR-laying' NAD+ into a nuclear signal. *Genes Dev*, *19*(17), 1951-1967. https://doi.org/10.1101/gad.1331805

Kim, S., Eun, H. S., & Jo, E. K. (2019). Roles of Autophagy-Related Genes in the Pathogenesis of Inflammatory Bowel Disease. *Cells*, *8*(1). https://doi.org/10.3390/cells8010077

Kim, S. I., Yeo, S. G., Gen, Y., Ju, H. R., Kim, S. H., & Park, D. C. (2019). Differences in autophagy-associated mRNAs in peritoneal fluid of patients with endometriosis and gynecologic cancers. *Eur J Obstet Gynecol Reprod Biol X*, *2*, 100016. https://doi.org/10.1016/j.eurox.2019.100016

Klionsky, D. J., Abdel-Aziz, A. K., Abdelfatah, S., Abdellatif, M., Abdoli, A., Abel, S., . . . Tong, C. K. (2021). Guidelines for the use and interpretation of assays for monitoring autophagy (4th edition). *Autophagy*, *17*(1), 1-382. https://doi.org/10.1080/15548627.2020.1797280

Lamark, T., Svenning, S., & Johansen, T. (2017). Regulation of selective autophagy: the p62/SQSTM1 paradigm. *Essays Biochem*, *61*(6), 609-624. https://doi.org/10.1042/EBC20170035

Lamb, C. A., Yoshimori, T., & Tooze, S. A. (2013). The autophagosome: origins unknown, biogenesis complex. *Nat Rev Mol Cell Biol*, *14*(12), 759-774. https://doi.org/10.1038/nrm3696

Lancaster, D. L., Patel, N., Lennard, L., & Lilleyman, J. S. (2002). Leucocyte versus erythrocyte thioguanine nucleotide concentrations in children taking thiopurines for acute lymphoblastic leukaemia. *Cancer Chemother Pharmacol*, *50*(1), 33-36. https://doi.org/10.1007/s00280-002-0442-6

Ledder, O., Lemberg, D. A., & Day, A. S. (2015). Thiopurine-induced pancreatitis in inflammatory bowel diseases. *Expert Rev Gastroenterol Hepatol*, *9*(4), 399-403. https://doi.org/10.1586/17474124.2015.992879

Li, F., Wang, L., Burgess, R. J., & Weinshilboum, R. M. (2008). Thiopurine S-methyltransferase pharmacogenetics: autophagy as a mechanism for variant allozyme degradation. *Pharmacogenet Genomics*, *18*(12), 1083-1094. https://doi.org/10.1097/FPC.0b013e328313e03f

Liu, B., Oltvai, Z. N., Bayır, H., Silverman, G. A., Pak, S. C., Perlmutter, D. H., & Bahar, I. (2017). Quantitative assessment of cell fate decision between autophagy and apoptosis. *Sci Rep*, *7*(1), 17605. https://doi.org/10.1038/s41598-017-18001-w

Liu, W. J., Ye, L., Huang, W. F., Guo, L. J., Xu, Z. G., Wu, H. L., . . . Liu, H. F. (2016). p62 links the autophagy pathway and the ubiqutin-proteasome system upon ubiquitinated protein degradation. *Cell Mol Biol Lett*, *21*, 29. https://doi.org/10.1186/s11658-016-0031-z

Machihara, K., & Namba, T. (2019). BAP31 Inhibits Cell Adaptation to ER Stress Conditions, Negatively Regulating Autophagy Induction by Interaction with STX17. *Cells*, *8*(11). https://doi.org/10.3390/cells8111350

McEwan, D. G., Popovic, D., Gubas, A., Terawaki, S., Suzuki, H., Stadel, D., . . . Dikic, I. (2015). PLEKHM1 regulates autophagosome-lysosome fusion through HOPS complex and LC3/GABARAP proteins. *Mol Cell*, *57*(1), 39-54. https://doi.org/10.1016/j.molcel.2014.11.006

Mikkelsen, T. S., Thorn, C. F., Yang, J. J., Ulrich, C. M., French, D., Zaza, G., . . . Altman, R. B. (2011). PharmGKB summary: methotrexate pathway. *Pharmacogenet Genomics*, *21*(10), 679-686. https://doi.org/10.1097/FPC.0b013e328343dd93

Mizushima, N., Yoshimori, T., & Levine, B. (2010). Methods in mammalian autophagy research. *Cell*, *140*(3), 313-326. https://doi.org/10.1016/j.cell.2010.01.028

Moriyama, T., Nishii, R., Perez-Andreu, V., Yang, W., Klussmann, F. A., Zhao, X., . . . Yang, J. J. (2016). NUDT15 polymorphisms alter thiopurine metabolism and hematopoietic toxicity. *Nat Genet*, *48*(4), 367-373. https://doi.org/10.1038/ng.3508

Myeku, N., & Figueiredo-Pereira, M. E. (2011). Dynamics of the degradation of ubiquitinated proteins by proteasomes and autophagy: association with sequestosome 1/p62. *J Biol Chem*, *286*(25), 22426-22440. https://doi.org/10.1074/jbc.M110.149252

Nakatogawa, H., Suzuki, K., Kamada, Y., & Ohsumi, Y. (2009). Dynamics and diversity in autophagy mechanisms: lessons from yeast. *Nat Rev Mol Cell Biol*, *10*(7), 458-467. https://doi.org/10.1038/nrm2708

Nguyen, C. M., Mendes, M. A., & Ma, J. D. (2011). Thiopurine methyltransferase (TPMT) genotyping to predict myelosuppression risk. *PLoS Curr*, *3*, RRN1236. https://doi.org/10.1371/currents.RRN1236

Novak, I., Kirkin, V., McEwan, D. G., Zhang, J., Wild, P., Rozenknop, A., . . . Dikic, I. (2010). Nix is a selective autophagy receptor for mitochondrial clearance. *EMBO Rep*, *11*(1), 45-51. https://doi.org/10.1038/embor.2009.256

Nunes, V., Cazzaniga, G., & Biondi, A. (2017). An update on PCR use for minimal residual disease monitoring in acute lymphoblastic leukemia. *Expert Rev Mol Diagn*, *17*(11), 953-963. https://doi.org/10.1080/14737159.2017.1377073

Ogata, M., Hino, S., Saito, A., Morikawa, K., Kondo, S., Kanemoto, S., . . . Imaizumi, K. (2006). Autophagy is activated for cell survival after endoplasmic reticulum stress. *Mol Cell Biol*, *26*(24), 9220-9231. https://doi.org/10.1128/MCB.01453-06

Oku, M., & Sakai, Y. (2018). Three Distinct Types of Microautophagy Based on Membrane Dynamics and Molecular Machineries. *Bioessays*, *40*(6), e1800008. https://doi.org/10.1002/bies.201800008

Olsvik, H. L., Lamark, T., Takagi, K., Larsen, K. B., Evjen, G., Øvervatn, A., . . . Johansen, T. (2015). FYCO1 Contains a C-terminally Extended, LC3A/B-preferring LC3-interacting Region (LIR) Motif Required for Efficient Maturation of Autophagosomes during Basal Autophagy. *J Biol Chem*, *290*(49), 29361-29374. https://doi.org/10.1074/jbc.M115.686915

Pankiv, S., Clausen, T. H., Lamark, T., Brech, A., Bruun, J. A., Outzen, H., . . . Johansen, T. (2007). p62/SQSTM1 binds directly to Atg8/LC3 to facilitate degradation of ubiquitinated protein aggregates by autophagy. *J Biol Chem*, *282*(33), 24131-24145. https://doi.org/10.1074/jbc.M702824200

Park, J. S., Oh, S. Y., Lee, D. H., Lee, Y. S., Sung, S. H., Ji, H. W., . . . Bae, S. H. (2016). p62/SQSTM1 is required for the protection against endoplasmic reticulum stress-induced apoptotic cell death. *Free Radic Res*, *50*(12), 1408-1421. https://doi.org/10.1080/10715762.2016.1253073

Park, K., Yoo, H. S., Oh, C. K., Lee, J. R., Chung, H. J., Kim, H. N., . . . Kim, D. W. (2022). Reciprocal interactions among Cobll1, PACSIN2, and SH3BP1 regulate drug resistance in chronic myeloid leukemia. *Cancer Med*. https://doi.org/10.1002/cam4.4727

Peng, Y., Qiu, L., Xu, D., Zhang, L., Yu, H., Ding, Y., . . . Lin, J. (2017). M. *Life Sci*, *185*, 63-72. https://doi.org/10.1016/j.lfs.2017.07.024

Queudeville, M., & Ebinger, M. (2021). Blinatumomab in Pediatric Acute Lymphoblastic Leukemia-From Salvage to First Line Therapy (A Systematic Review). *J Clin Med*, *10*(12). https://doi.org/10.3390/jcm10122544

Rabanal-Ruiz, Y., Otten, E. G., & Korolchuk, V. I. (2017). mTORC1 as the main gateway to autophagy. *Essays Biochem*, *61*(6), 565-584. https://doi.org/10.1042/EBC20170027

Rao, Y., Ma, Q., Vahedi-Faridi, A., Sundborger, A., Pechstein, A., Puchkov, D., . . . Haucke, V. (2010). Molecular basis for SH3 domain regulation of F-BAR-mediated membrane deformation. *Proc Natl Acad Sci U S A*, *107*(18), 8213-8218. https://doi.org/10.1073/pnas.1003478107

Relling, M. V., & Evans, W. E. (2015). Pharmacogenomics in the clinic. *Nature*, *526*(7573), 343-350. https://doi.org/10.1038/nature15817

Relling, M. V., Schwab, M., Whirl-Carrillo, M., Suarez-Kurtz, G., Pui, C. H., Stein, C. M., . . . Yang, J. J. (2019). Clinical Pharmacogenetics Implementation Consortium Guideline for Thiopurine

Dosing Based on TPMT and NUDT15 Genotypes: 2018 Update. *Clin Pharmacol Ther*, *105*(5), 1095-1105. https://doi.org/10.1002/cpt.1304

Riello, L., Talbotec, C., Garnier-Lengliné, H., Pigneur, B., Svahn, J., Canioni, D., . . . Ruemmele, F. M. (2011). Tolerance and efficacy of azathioprine in pediatric Crohn's disease. *Inflamm Bowel Dis*, *17*(10), 2138-2143. https://doi.org/10.1002/ibd.21612

Rozenknop, A., Rogov, V. V., Rogova, N. Y., Löhr, F., Güntert, P., Dikic, I., & Dötsch, V. (2011). Characterization of the interaction of GABARAPL-1 with the LIR motif of NBR1. *J Mol Biol*, *410*(3), 477-487. https://doi.org/10.1016/j.jmb.2011.05.003

Ruemmele, F. M., Veres, G., Kolho, K. L., Griffiths, A., Levine, A., Escher, J. C., . . . European Society of Pediatric Gastroenterology, H. p. a. N. (2014). Consensus guidelines of ECCO/ESPGHAN on the medical management of pediatric Crohn's disease. *J Crohns Colitis*, *8*(10), 1179-1207. https://doi.org/10.1016/j.crohns.2014.04.005

Schaaf, M. B., Keulers, T. G., Vooijs, M. A., & Rouschop, K. M. (2016). LC3/GABARAP family proteins: autophagy-(un)related functions. *FASEB J*, *30*(12), 3961-3978. https://doi.org/10.1096/fj.201600698R

Seinen, M. L., van Nieuw Amerongen, G. P., de Boer, N. K., & van Bodegraven, A. A. (2016). Rac Attack: Modulation of the Small GTPase Rac in Inflammatory Bowel Disease and Thiopurine Therapy. *Mol Diagn Ther*, *20*(6), 551-557. https://doi.org/10.1007/s40291-016-0232-1

Senju, Y., Itoh, Y., Takano, K., Hamada, S., & Suetsugu, S. (2011). Essential role of PACSIN2/syndapin-II in caveolae membrane sculpting. *J Cell Sci*, *124*(Pt 12), 2032-2040. https://doi.org/10.1242/jcs.086264

Senju, Y., Rosenbaum, E., Shah, C., Hamada-Nakahara, S., Itoh, Y., Yamamoto, K., . . . Suetsugu, S. (2015). Phosphorylation of PACSIN2 by protein kinase C triggers the removal of caveolae from the plasma membrane. *J Cell Sci*, *128*(15), 2766-2780. https://doi.org/10.1242/jcs.167775

Sin, C. F., & Man, P. M. (2021). The Role of Proteasome Inhibitors in Treating Acute Lymphoblastic Leukaemia. *Front Oncol*, *11*, 802832. https://doi.org/10.3389/fonc.2021.802832

Smid, A., Karas-Kuzelicki, N., Jazbec, J., & Mlinaric-Rascan, I. (2016). PACSIN2 polymorphism is associated with thiopurine-induced hematological toxicity in children with acute lymphoblastic leukaemia undergoing maintenance therapy. *Sci Rep*, *6*, 30244. https://doi.org/10.1038/srep30244

Sousa, P., Estevinho, M. M., Dias, C. C., Ministro, P., Kopylov, U., Danese, S., . . . Magro, F. (2020). Thiopurines' Metabolites and Drug Toxicity: A Meta-Analysis. *J Clin Med*, *9*(7). https://doi.org/10.3390/jcm9072216

Stocco, G., Yang, W., Crews, K. R., Thierfelder, W. E., Decorti, G., Londero, M., . . . Evans, W. E. (2012). PACSIN2 polymorphism influences TPMT activity and mercaptopurine-related gastrointestinal toxicity. *Hum Mol Genet*, *21*(21), 4793-4804. https://doi.org/10.1093/hmg/dds302

Suarez-Kurtz, G., Araújo, G. S., & de Sousa, S. J. (2020). Pharmacogeomic implications of population diversity in Latin America: TPMT and NUDT15 polymorphisms and thiopurine dosing. *Pharmacogenet Genomics*, *30*(1), 1-4. https://doi.org/10.1097/FPC.0000000000000388

Suiter, C. C., Moriyama, T., Matreyek, K. A., Yang, W., Scaletti, E. R., Nishii, R., . . . Yang, J. J. (2020). Massively parallel variant characterization identifies. *Proc Natl Acad Sci U S A*, *117*(10), 5394-5401. https://doi.org/10.1073/pnas.1915680117

Szyniarowski, P., Corcelle-Termeau, E., Farkas, T., Høyer-Hansen, M., Nylandsted, J., Kallunki, T., & Jäättelä, M. (2011). A comprehensive siRNA screen for kinases that suppress macroautophagy in optimal growth conditions. *Autophagy*, *7*(8), 892-903. https://doi.org/10.4161/auto.7.8.15770

Tai, H. L., Fessing, M. Y., Bonten, E. J., Yanishevsky, Y., d'Azzo, A., Krynetski, E. Y., & Evans, W. E. (1999). Enhanced proteasomal degradation of mutant human thiopurine S-methyltransferase (TPMT) in mammalian cells: mechanism for TPMT protein deficiency inherited by TPMT*2, TPMT*3A, TPMT*3B or TPMT*3C. *Pharmacogenetics*, *9*(5), 641-650. https://doi.org/10.1097/01213011-199910000-00011

Tanida, I., Ueno, T., & Kominami, E. (2008). LC3 and Autophagy. *Methods Mol Biol*, *445*, 77-88. https://doi.org/10.1007/978-1-59745-157-4_4

Terwilliger, T., & Abdul-Hay, M. (2017). Acute lymphoblastic leukemia: a comprehensive review and 2017 update. *Blood Cancer J*, *7*(6), e577. https://doi.org/10.1038/bcj.2017.53

Tiede, I., Fritz, G., Strand, S., Poppe, D., Dvorsky, R., Strand, D., . . . Neurath, M. F. (2003). CD28-dependent Rac1 activation is the molecular target of azathioprine in primary human CD4+ T lymphocytes. *J Clin Invest*, *111*(8), 1133-1145. https://doi.org/10.1172/JCI16432

Toksvang, L. N., Schmidt, M. S., Arup, S., Larsen, R. H., Frandsen, T. L., Schmiegelow, K., & Rank, C. U. (2019). Hepatotoxicity during 6-thioguanine treatment in inflammatory bowel disease

and childhood acute lymphoblastic leukaemia: A systematic review. *PLoS One*, *14*(5), e0212157. https://doi.org/10.1371/journal.pone.0212157

Tominaga, K., Sugaya, T., Tanaka, T., Kanazawa, M., Iijima, M., & Irisawa, A. (2020). Thiopurines: Recent Topics and Their Role in the Treatment of Inflammatory Bowel Diseases. *Front Pharmacol*, *11*, 582291. https://doi.org/10.3389/fphar.2020.582291

Tooze, J., Hollinshead, M., Ludwig, T., Howell, K., Hoflack, B., & Kern, H. (1990). In exocrine pancreas, the basolateral endocytic pathway converges with the autophagic pathway immediately after the early endosome. *J Cell Biol*, *111*(2), 329-345. https://doi.org/10.1083/jcb.111.2.329

Turner, D., Ruemmele, F. M., Orlanski-Meyer, E., Griffiths, A. M., de Carpi, J. M., Bronsky, J., . . . Russell, R. K. (2018). Management of Paediatric Ulcerative Colitis, Part 1: Ambulatory Care-An Evidence-based Guideline From European Crohn's and Colitis Organization and European Society of Paediatric Gastroenterology, Hepatology and Nutrition. *J Pediatr Gastroenterol Nutr*, *67*(2), 257-291. https://doi.org/10.1097/MPG.0000000000002035

van Hoeve, K., & Vermeire, S. (2020). Thiopurines in Pediatric Inflammatory Bowel Disease: Current and Future Place. *Paediatr Drugs*, *22*(5), 449-461. https://doi.org/10.1007/s40272-020-00411-5

Virág, L. (2005). Structure and function of poly(ADP-ribose) polymerase-1: role in oxidative stress-related pathologies. *Curr Vasc Pharmacol*, *3*(3), 209-214. https://doi.org/10.2174/1570161054368625

Vodenkova, S., Buchler, T., Cervena, K., Veskrnova, V., Vodicka, P., & Vymetalkova, V. (2020). 5-fluorouracil and other fluoropyrimidines in colorectal cancer: Past, present and future. *Pharmacol Ther*, *206*, 107447. https://doi.org/10.1016/j.pharmthera.2019.107447

Wang, L., Li, J., Shi, X., Li, S., Tang, P. M., Li, Z., . . . Wei, C. (2019). Antimalarial Dihydroartemisinin triggers autophagy within HeLa cells of human cervical cancer through Bcl-2 phosphorylation at Ser70. *Phytomedicine*, *52*, 147-156. https://doi.org/10.1016/j.phymed.2018.09.221

Wang, Y., Kim, N. S., Haince, J. F., Kang, H. C., David, K. K., Andrabi, S. A., . . . Dawson, T. M. (2011). Poly(ADP-ribose) (PAR) binding to apoptosis-inducing factor is critical for PAR polymerase-1-dependent cell death (parthanatos). *Sci Signal*, *4*(167), ra20. https://doi.org/10.1126/scisignal.2000902

Whirl-Carrillo, M., McDonagh, E. M., Hebert, J. M., Gong, L., Sangkuhl, K., Thorn, C. F., . . . Klein, T. E. (2012). Pharmacogenomics knowledge for personalized medicine. *Clin Pharmacol Ther*, *92*(4), 414-417. https://doi.org/10.1038/clpt.2012.96

Wirth, M., Zhang, W., Razi, M., Nyoni, L., Joshi, D., O'Reilly, N., . . . Mouilleron, S. (2019). Molecular determinants regulating selective binding of autophagy adapters and receptors to ATG8 proteins. *Nat Commun*, *10*(1), 2055. https://doi.org/10.1038/s41467-019-10059-6

Xie, Q., Liu, Y., & Li, X. (2020). The interaction mechanism between autophagy and apoptosis in colon cancer. *Transl Oncol*, *13*(12), 100871. https://doi.org/10.1016/j.tranon.2020.100871

Yates, C. R., Krynetski, E. Y., Loennechen, T., Fessing, M. Y., Tai, H. L., Pui, C. H., . . . Evans, W. E. (1997). Molecular diagnosis of thiopurine S-methyltransferase deficiency: genetic basis for azathioprine and mercaptopurine intolerance. *Ann Intern Med*, *126*(8), 608-614. https://doi.org/10.7326/0003-4819-126-8-199704150-00003

Yorimitsu, T., & Klionsky, D. J. (2005). Autophagy: molecular machinery for self-eating. *Cell Death Differ*, *12 Suppl 2*, 1542-1552. https://doi.org/10.1038/sj.cdd.4401765

Yoshii, S. R., & Mizushima, N. (2017). Monitoring and Measuring Autophagy. *Int J Mol Sci*, *18*(9). https://doi.org/10.3390/ijms18091865

Zaza, G., Cheok, M., Krynetskaia, N., Thorn, C., Stocco, G., Hebert, J. M., . . . Altman, R. B. (2010). Thiopurine pathway. *Pharmacogenet Genomics*, *20*(9), 573-574. https://doi.org/10.1097/FPC.0b013e328334338f

Zhang, C., Yu, X., Gao, J., Zhang, Q., Sun, S., Zhu, H., . . . Yan, H. (2018). PINK1/Parkin-mediated mitophagy was activated against 1,4-Benzoquinone-induced apoptosis in HL-60 cells. *Toxicol In Vitro*, *50*, 217-224. https://doi.org/10.1016/j.tiv.2018.03.002

Zhao, Y. G., & Zhang, H. (2019). Autophagosome maturation: An epic journey from the ER to lysosomes. *J Cell Biol*, *218*(3), 757-770. https://doi.org/10.1083/jcb.201810099

Zhu, F., Li, X., Tang, X., Jiang, J., Han, Y., Li, Y., . . . He, Y. (2021). Neferine promotes the apoptosis of HNSCC through the accumulation of p62/SQSTM1 caused by autophagic flux inhibition. *Int J Mol Med*, *48*(1). https://doi.org/10.3892/ijmm.2021.4957

Zoncu, R., Bar-Peled, L., Efeyan, A., Wang, S., Sancak, Y., & Sabatini, D. M. (2011). mTORC1 senses lysosomal amino acids through an inside-out mechanism that requires the vacuolar H(+)-ATPase. *Science*, *334*(6056), 678-683. https://doi.org/10.1126/science.1207056